TECHNICAL REPORT

Bending tests on glulam-CLT beams connected with double-sided punched metal plate fasteners and inclined screws

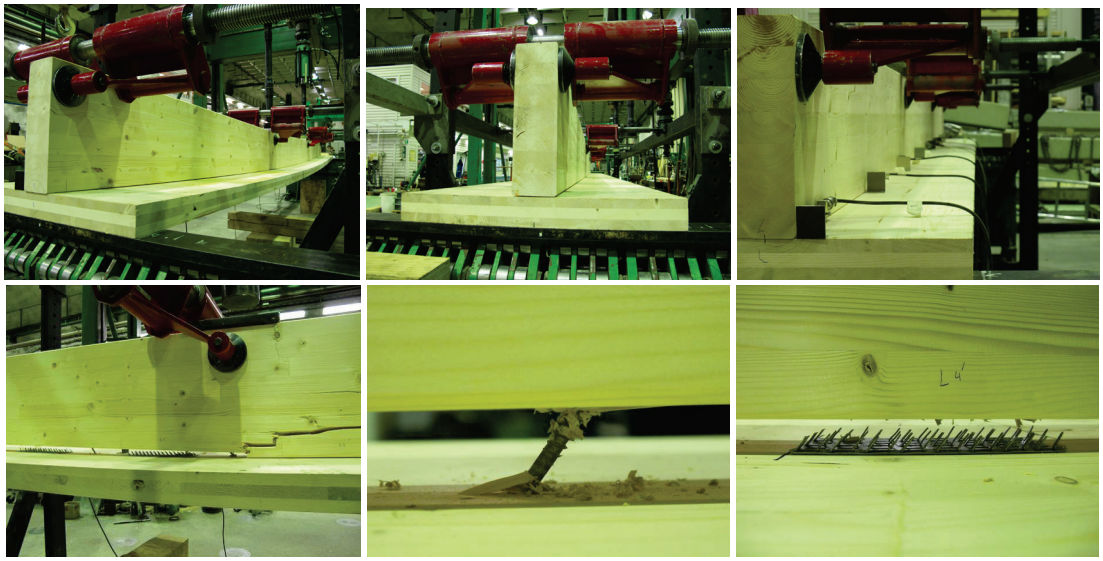

Nicolas Jacquier

LULEÅ UNIVERSITY OF TECHNOLOGY

ISSN 1402-1536
ISBN 978-91-7583-212-8 (pdf)

Luleå 2015

www.ltu.se

LULEÅ UNIVERSITY OF TECHNOLOGY

Bending tests on glulam-CLT beams Connected with double-sided punched metal plate fasteners and inclined screws

Nicolas Jacquier

Luleå University of Technology
Department of Civil, Environmental and Natural Resources Engineering
Division of Structural and Construction Engineering

Abstract

This report presents bending tests performed on composite beams made from glulam beams and cross laminated timber (CLT) panels. The composite beam, with a T-cross section, represents a section of a floor element in a multi-storey CLT construction system. The shear connections used were made either of double-sided punched metal plate fasteners, either of inclined screws, or of a combination of both fastener types. The screws are used to secure the shear connection with double-sided nail plates with respect to possible separation forces between the glulam and the CLT. An additional test with a screw glued connection was made for comparison as the upper bound case in terms of composite action. The results show the beams with double-sided nail plates (with or without screws) achieved a very high level of composite action and an overall satisfactory behaviour. Almost full composite action was achieved for the screw-glued composite beam. A detailed design example of the beam element according to the Eurocode 5 and Finnish National Annex is presented.

Table of Contents

1 Introduction

A composite timber floor made with glulam and Cross Laminated Timber (CLT) and its shear connection system are investigated in a bending situation. An example of glulam-CLT cassette floor element with CLT at the bottom is shown in Fig. 1 and is a possible floor configuration considered in a residential multi-storey CLT construction system. Only the CLT panel and the glulam beams are load bearing. The shear connection considered is made of double-sided punched metal plate fasteners in combination with inclined screws.

The behaviour of joints with double-sided nail plates (DSNP) and inclined screws combined was evaluated under shear tests [1]. The screws are used to compensate the lack of withdrawal resistance of the double-sided nail plates and to improve the overall joint behaviour (strength, stiffness and post peak-load behaviour). More background information and motivation for this study is presented in [1] and [2].

The aim of the study is to evaluate the performance (strength, stiffness, behaviour) of composite timber beam elements with DSNP shear connectors and to evaluate the influence of additional screws on the overall beam performance. The study intends to evaluate the technical feasibility of a particular design of a glulam-CLT composite floor made with such shear connectors by proposing and testing a likely design of a floor element of 6.4 m span, for which a detailed design example is presented in Appendix A.

The experimental program presented in this report also considers the combination of double-sided nail plates and inclined screws. Three bending tests series (of 3 test specimens each) with different arrangements of mechanical fasteners (DSNP and screws) were performed on glulam-CLT beam elements assembled with either:

- double-sided nail plate (DSNP) fasteners;
- inclined (45°) self-tapping screws;
- double-sided nail plates (DSNP) combined with inclined (45°) self-tapping screws.

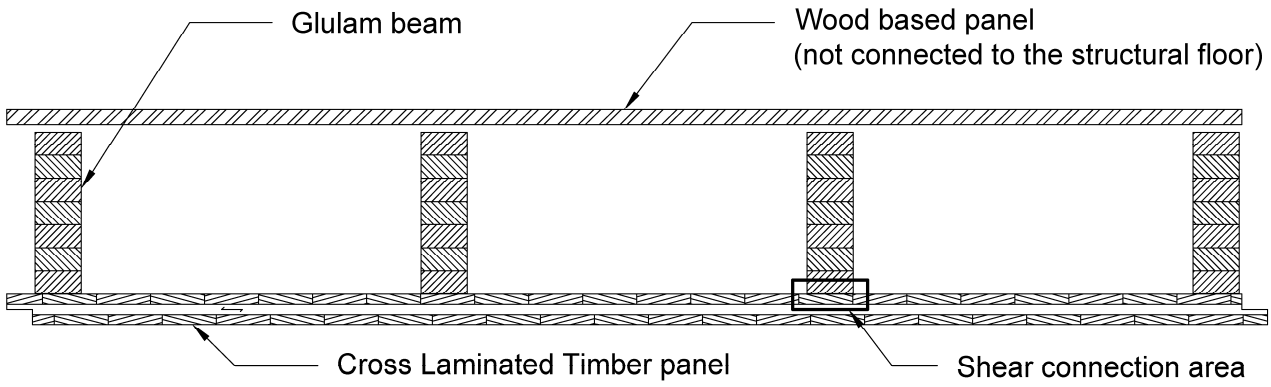

Fig. 1: Example of a glulam-CLT cassette floor element with CLT panel located at the bottom.

2 Methods

The experimental test program was carried at the laboratories of VTT Expert Services Ltd in Finland. Three series (of 3 specimens each) of glulam-CLT composite beams connected with mechanical fasteners were tested under 4-point bending tests corresponding to a likely design of a floor element in order to investigate the behaviour and performance of different shear connection configurations. An additional single bending test was performed on a screw-glued composite beam in order to compare beams connected with mechanical fasteners and beams with a glued shear connection and therefore an assumed full composite action. The beams were 6.5 meter long and had the same cross-section, shown in Fig. 2 for the case of a connection with combined double-sided nail plate and inclined screw. This cross-section corresponds to the total floor element presented in Fig. 1 reduced to a single beam element.

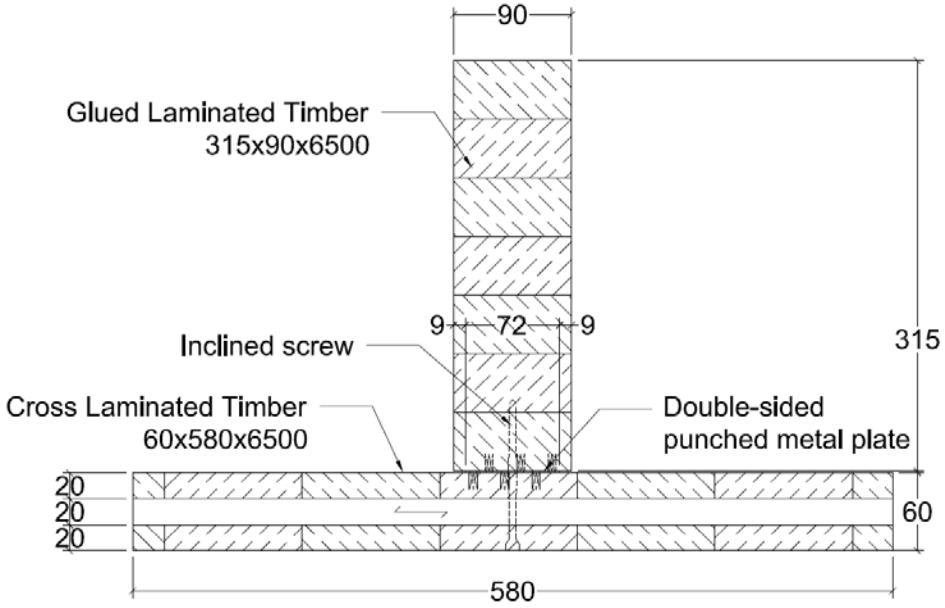

Fig. 2: Cross section of the composite glulam-CLT beam with double-sided nail plate and inclined screw shear connection (dimensions in mm).

2.1 Shear connectors

The shear connectors considered are double-sided punched metal plate fasteners (Fig. 3) and self-tapping screws (Fig. 4). The configurations of the shear connectors in the different test series is given in section 2.4.

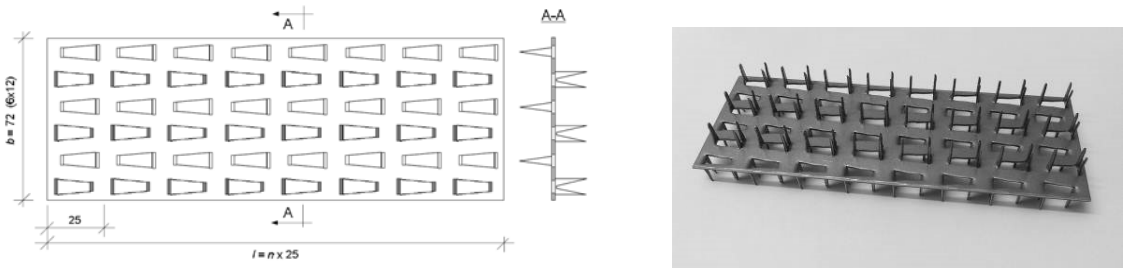

Fig. 3: Double-sided punched metal plate Sepa-SE2P, (dimensions b_{NP} × l_{NP}) 72 × 200 mm^2.

The double-sided punched metal plate fasteners Sepa-SE2P (Fig. 3) are made of zinc coated steel with dimensions ($b_{NP} \times l_{NP}$) 72×200 mm^2, steel plate thickness 1.3 mm and teeth length 15.6 mm. Mechanical properties (mean values) according to the manufacturing's inspection certificate are: tensile yield strength f_y = 410 N/mm^2, ultimate tensile strength f_u = 485 N/mm^2, elongation ε_u = 28.0 % and weight of zinc coating 293 g/m^2.

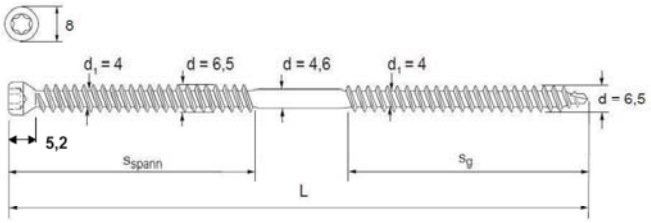

Fig. 4: SFS-Intec WT-T screw geometry with diameter 6.5 mm (source SFS Intec [3]).

SFS Intec WT-T self-drilling screws (Fig. 4) are used in series with inclined screws. The screw nominal dimensions ($d \times L$ in mm) 6.5 × 160 (thread length s_g 65 mm) and properties are according to the European Technical Approval ETA-12/0063 [3].

The load-carrying capacity and slip modulus for the individual shear connectors obtained from shear tests on glulam-CLT joints [1] are reported in Table 1.

Table 1: Load-carrying capacity, slip modulus and specific slip values for single shear connectors [1].

Shear connector type (Test series name as reported in [1])	Load-carrying capacity	Slip modulus	Yield slip	Slip at maximum load
	F_{max} (CoV) kN (%)	k_s (CoV) kN/mm (%)	u_y (CoV) mm (%)	u_{max} (CoV) mm (%)
Screw SFS-WT-T 6.5×160 inclined at α = 45° (S1_2S-6.5)	8.0 (5.3)	9.7 (7.3)	0.67 (19.9)	1.78 (9.4)
Double-sided nail plate Sepa-SE2P (S8_1NP-200)	32.9 (2.9)	53.6 (7.8)	0.27 (1.4)	5.26 (8.8)

A one-component polyurethane glue Purbond HB110 (250 gr/m2) was used for the screw-glued specimen. Vertical SFS Intec screws WFD-T-H12-8×180 were used with 28 mm diameter washers (Fig. 5) to apply the necessary pressure on the glue line. Dimensions *d*, *L1*, and *L2* in Fig. 5 are 8 mm, 180mm, and 108 mm, respectively.

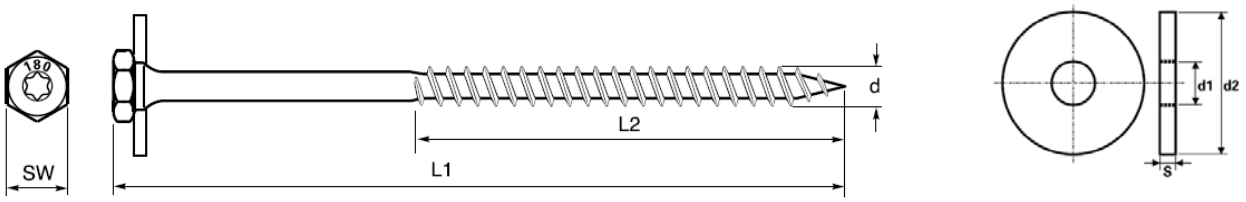

(a) (b)

Fig. 5: Screw and washer used for screw-gluing: (a) SFS Intec WFD-T-H12-8×180; (b) 28 mm washer (source SFS Intec [4]).

2.2 Glulam and CLT members

The glulam used was made of Norway Spruce (Picea abies) and labelled L40 (Nordic glulam strength class) and GL32 [5]. The glulam beams of length 6500 mm had a cross section of 90×315 mm^2 with glulam lamellas thickness of 45 mm. The CLT was manufactured from solid wood lamellas of strength class C24 according to European Technical Approval ETA-08/0271 [6], composed of three 20 mm thick layers with the outer ply grain oriented parallel to the span direction. The CLT panels of length 6500 mm had a cross section of 60×580 mm^2.

The global modulus of elasticity (MOE) according to EN 408 [7] was measured on three glulam beams and three CLT panels by 4-point bending load test up to $0.4\times F_{max,est}$,with $F_{max,est}$ taken equal to 18 kN and 3 kN for the glulam beams and the CLT panels, respectively.

The global MOE obtained for the glulam was $E_{global,glulam}$ = 11 898 N/mm^2 when neglecting the shear deformation. When considering the deflection due to shear deformation and assuming a shear modulus of 850 N/mm^2 according to the GL32h strength class, the estimated MOE was $E_{global,glulam,shear}$ = 12 290 N/mm^2.

Regarding the CLT the vertical shear deformation is neglected for the CLT as the span is very large in comparison to the CLT layers thicknesses. The global MOE of the longitudinal layers was estimated using the "γ -method" (cf. section 2.3.1), considering the contribution of the top and bottom layers only and the rolling shear deformation in the traverse layer with a rolling shear modulus G_R = 50 N/mm^2 [8], giving $E_{global,CLT}$ = 11 445 N/mm^2 for the longitudinal CLT layers.

In this test report the values $E_{global,glulam}$ = 11 898 N/mm^2 and $E_{global,CLT}$ = 11 445 N/mm^2 are considered as the measured MOE of the glulam and CLT members, respectively.

2.3 Design method

The floor element investigated is intended to be used in Finland. The design of the composite beam element was therefore made according to the Eurocode 5 [9] and Finnish National Annex [10], and using preliminary test results for the shear connectors. The test specimens represent a likely design of a floor element which could be used in Finland. A detailed design example of the beam element is presented in Appendix A.

2.3.1 Design of the mechanically jointed glulam-CLT beam according to the γ-method

In the Eurocode 5, the design of mechanically jointed timber beams can be done with the so-called "*γ*-method". It is generally accepted that the design of horizontal CLT members in bending can also be done with the γ-method considering that only the longitudinal layers are load-carrying, and that the perpendicular ones act as flexible shear connections [11], [8]. In the γ-method, the ratio s/k in the usual expression of the γ factor, see Eq. (2), where s_1 [m] is the spacing of the individual mechanical fasteners and k_1 [kN/m] is the slip modulus of an individual mechanical fastener [N/m], should be replaced by the ratio $h/(G_R \times b)$, see Eq. (3), where h_{23} [m] is the thickness of the perpendicular CLT layer (here between the sub-element 2 and 3), G_R [N/m^2] is the rolling shear modulus and b_{23} [m] is the width of the perpendicular CLT layer (usually, as it is the case here $b_{23} = b_2 = b_3$).

The γ-method can be used for composite cross-sections up to three layers (with two flexible layers), and it can therefore be used for the glulam-CLT composite beam presented in this report. It should be noted that other methods allow to take into account the shear deformations in the CLT and to treat structures with more than three layers. These methods are not presented in the Eurocode 5 and do not permit to carry out simple hand calculation. They are therefore out of the scope of the present design procedure description.

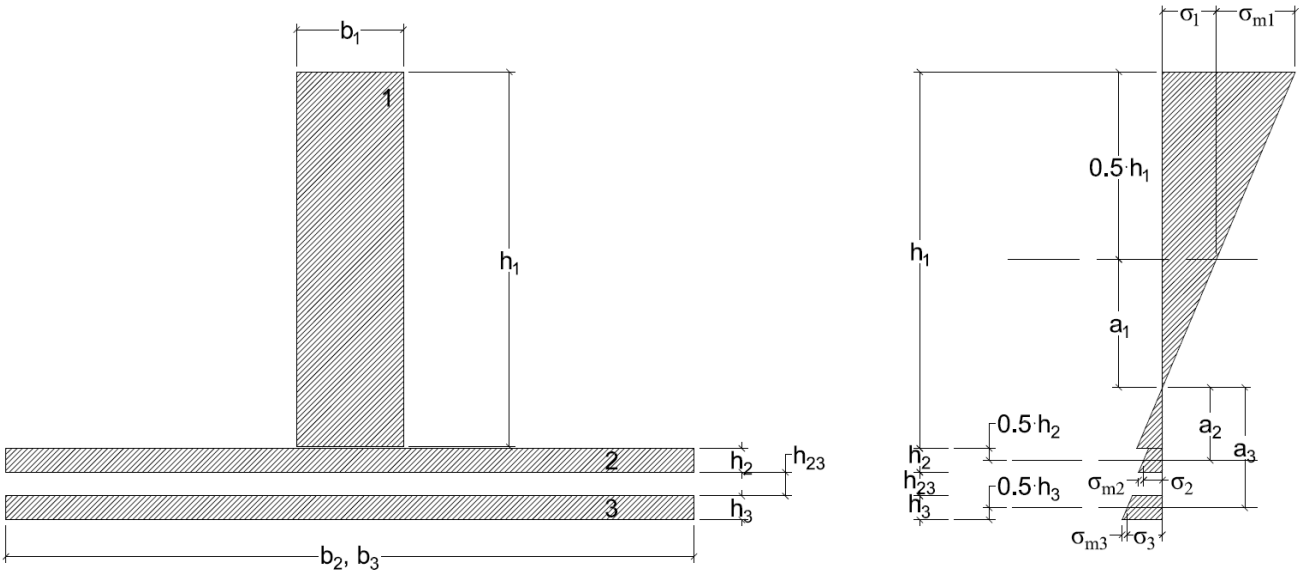

Fig. 6: Glulam-CLT cross-section and stress diagram with the notation considered in the γ-method.

The effective bending stiffness EI_{ef} of the composite glulam-CLT beam element is calculated as follows:

$$EI_{ef} = \sum_{i=1}^{3} (E_i I_i + \gamma_i E_i A_i a_i^2) \tag{1}$$

where E_i, A_i and I_i are the modulus of elasticity, the area and the second moment of area of the i^{th} sub-element in Fig. 6, respectively, $\gamma_2 = 1$ and where:

$$\gamma_1 = \left(1 + \pi^2 \frac{E_1 A_1 s_1}{k_1 L^2} \right)^{-1} \tag{2}$$

$$\gamma_3 = \left(1 + \pi^2 \frac{E_3 A_3 h_{23}}{G_R b_{23} L^2} \right)^{-1} \tag{3}$$

$$a_2 = \frac{\gamma_1 E_1 A_1 \left(\frac{h_1 + h_2}{2} \right) - \gamma_3 E_3 A_3 \left(\frac{h_2 + h_3}{2} + h_{23} \right)}{\gamma_1 E_1 A_1 + \gamma_2 E_2 A_2 + \gamma_3 E_3 A_3} \tag{4}$$

$$a_1 = \frac{h_1 + h_2}{2} - a_2 \tag{5}$$

$$a_3 = \frac{h_2 + h_3}{2} + h_{23} + a_2 \tag{6}$$

where s_1 and k_1 are the spacing and the slip modulus, respectively, of the individual shear connectors between the sub-element 1 and 2, and h_1, h_2, h_3 and h_{23} are the respective heights of the different sub-elements according to Fig. 6.

The normal stress σ_i and bending stress $\sigma_{m,i}$ in each sub-element, Eq. (7) and Eq. (8), respectively, and the force F_1 in a single shear connector, Eq. (9), can be calculated according to the expressions given in the Eurocode 5:

$$\sigma_i = \frac{\gamma_i E_i a_i}{EI_{ef}} M \tag{7}$$

$$\sigma_{m,i} = \frac{0.5 E_i h_i}{EI_{ef}} M \tag{8}$$

where M is the external moment at the position of interest and h_i is the height of the sub-element evaluated;

$$F_1 = \frac{\gamma_1 E_1 A_1 a_1 s_1}{EI_{ef}} V \tag{9}$$

where V is the total shear force at the position of the fastener considered.

Conservatively, it can be assumed for the shear stress verification in the glulam that the glulam beam resists the entire shear force as suggested in [12] for the design of a LVL-concrete composite structure using Eq. (10):

$$\tau_{1,\max} = 1.5\frac{V}{A_1} \tag{10}$$

where V is the total shear force at the position considered.

The verification which must be carried out in the CLT with respect to the shear force concerns the transverse layer with the verification of the rolling shear stresses, the rolling shear strength being much lower than the shear strength for the layers loaded parallel. The rolling shear stresses in the cross-layer can be calculated by assuming a constant uniform shear stress distribution over this layer equal to the shear stress level at the interface between the sub-elements 2 and 3 with Eq. (11):

$$\tau_{v,23} = \frac{\gamma_3 E_3 A_3 a_3}{EI_{ef} b_3} V \tag{11}$$

A more conservative assumption is to consider that the shear stresses are distributed from the glulam beam down to the perpendicular layer with a 45° angle distribution, therefore virtually reducing the resisting width of the cross-layer. The rolling shear stress could therefore alternatively (alt) be calculated with Eq. (12):

$$\tau_{v,23,\text{alt}} = \frac{\gamma_3 E_3 A_3 a_3}{EI_{ef} (b_1 + 2h_2)} V \tag{12}$$

2.3.2 Serviceability design criteria

The Finnish National Annex [13] of the Eurocode 5 [9] specifies that timber floors should have a fundamental frequency of at least 9 Hz or that a special investigation should be carried out. It is suggested that for simply supported floors on only two sides, the fundamental frequency can be calculated with Eq. (13):

$$f_1 = \frac{\pi}{2 \cdot L^2} \sqrt{\frac{(EI)_l}{m}} \tag{13}$$

where L is the floor span, $(EI)_l$ is the equivalent plate bending stiffness of the floor about an axis perpendicular to the span direction [Nm^2/m], and m is the mass of the floor to consider calculated as $m = m_G + 30$ kg/m^2, where m_G is the self-weight of the finished floor element and where the term 30 kg/m^2 accounts for the permanent part of the service load [14]. The Finnish National Annex formerly specified to calculate the contributing floor mass as $m = m_G + \psi_2 q_k$ with ψ_2 the partial coefficient for the quasi-permanent load combination and q_k the characteristic service load for the floor.

The Finnish National Annex also recommends that floors having a fundamental frequency higher than 9 Hz should also verify that the maximum deflection δ_{1kN} (Eq. (14)) caused by a static concentrated loading P = 1 kN should not exceed 0.5 mm, calculated:

$$\delta_{1kN} = \min\left\{ \frac{PL^2}{42 \cdot k_\delta \cdot (EI)_l} \; ; \; \frac{PL^3}{42 \cdot s \cdot (EI)_l} \right\} \tag{14}$$

where k_δ (Eq. (15)) is a coefficient accounting for the distribution of the concentrated load over the floor width depending on the bending stiffness of the floor with respect to an axis parallel to the span direction $(EI)_b$ [Nm^2/m], B is the floor width, and s the spacing of the floor beams.

$$k_\delta = \min\left\{ \frac{B}{L} \; ; \; \sqrt[4]{\frac{(EI)_l}{(EI)_b}} \right\} \tag{15}$$

The contribution of the additional floor finishes layers (i.e. floating floor) can be considered in addition for the transverse bending stiffness $(EI)_b$ and can allow to distribute even more the concentrated load over the floor width.

The unit impulse velocity response v [m/(N·s^2)] according to Eqs. (16) and (17) should verify $v \le b^{(f_1 \zeta - 1)}$, where according to the Finnish National Annex b = 150 and ζ is the modal damping ratio of the floor.

$$v = \frac{4(0.4 + 0.6 n_{40})}{m \cdot B \cdot L + 200} \tag{16}$$

$$n_{40} = \left\{ \left(\left(\frac{40}{f_1} \right)^2 - 1 \right) \left(\frac{B}{L} \right)^4 \frac{(EI)_l}{(EI)_b} \right\}^{0.25} \tag{17}$$

2.4 Test series

The test series are described in Table 2 and Fig. 7. The shear connection of the specimens of the series B2_NP (double-sided nail plates only) and B3_NP+S (double-sided nail plates and screws combined) were designed so that the finished floor would have a fundamental frequency of at least 9 Hz for a load case consisting of a uniformly distributed permanent load G_k = 1.8 kN/m^2 and a service load Q_k = 2 kN/m^2. The beam B1_S was under-designed with a minimal shear connection made with a small amount of screw as the lower bound case from a composite action point of view. A constant spacing of the connectors along the beam s = 450 mm was used in all series except for the single test made with screw-gluing where the spacing between vertical screws was 200 mm, representing the upper bound case aiming for full composite action.

Table 2: Description of the test series: screws only (B1_S), double-sided nail plates only (B2_NP), double-sided nail plates and screws combined (B3_NP+S), and screw-gluing (B4_SG).

			Spacing s = 450 mm		Spacing s = 200 mm
Test series Name	**No. of tests**	**Estimated load F_{est} (kN)**	**Screws inclined at 45° (shear tension) $d \times l_s$ (mm)**	**Double-sided nail plates $b_{NP} \times l_{NP}$ (mm)**	**Vertical screws for screw-gluing $d \times l_s$ (mm)**
B1_S	3	75	6.5 × 160	-	-
B2_NP	3	75	-	72 × 200	-
B_NP+S	3	90	6.5 × 160	72 × 200	-
B4_SG	1	110	-	-	8 × 180

d is the nominal screw diameter, l_s is the screw length, b_{NP} and l_{NP} are the DSNP width and length, respectively.

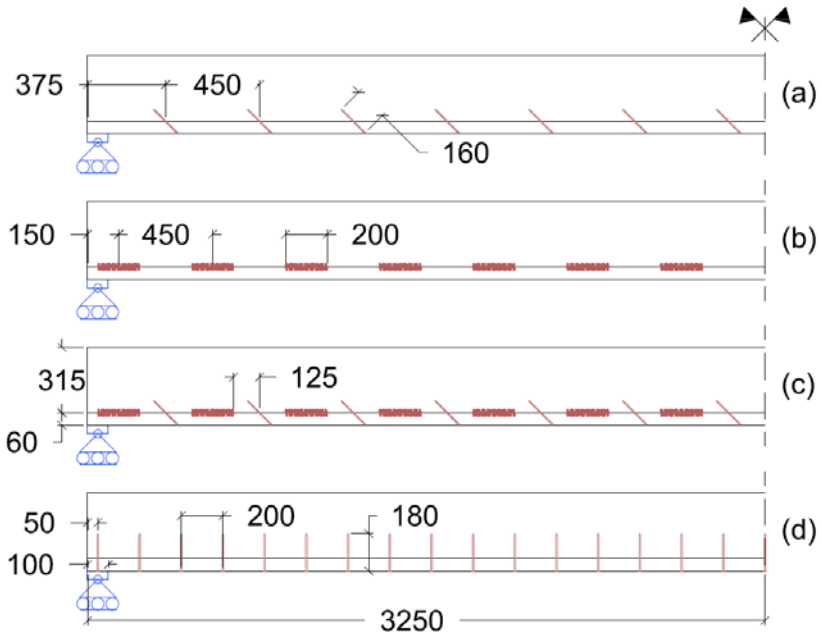

Fig. 7: Configuration of the test series: (a) screws only (B1_S), (b) double-sided nail plates only (B2_NP), (c) double-sided nail plates and screws (B3_ NP+S), (d) screw-gluing (B4_SG).

2.5 Preparation, conditioning and assembly

The timber members were stored at 65 % relative humidity (RH) and 20 °C temperature (T) for 8 at least weeks before assembly. After assembly with the double-sided nail plates fasteners, the composite beams were stored again in the climate controlled room under the same conditions for 4 weeks before the bending tests.

The beam elements with double-sided nail plates were assembled in two steps in the laboratory by pressing first each double-sided nail plate individually into the CLT panel using a steel comb for double-sided nail plate (Fig. 8) and a load-controlled hydraulic jack with 55 kN per double-sided nail plate. After the installation of all the nail plates of the specimen in the CLT, the glulam beam was pressed onto the CLT panel using two hydraulic jacks applying each a force on a steel beam distributing the load over the glulam beam length (Fig. 9). A total load of 770 kN was applied on the glulam beam to press simultaneously the 14 double-sided nail plates of each test specimen.

Fig. 8: Positioning and pressing the double-sided nail plates on the CLT panel.

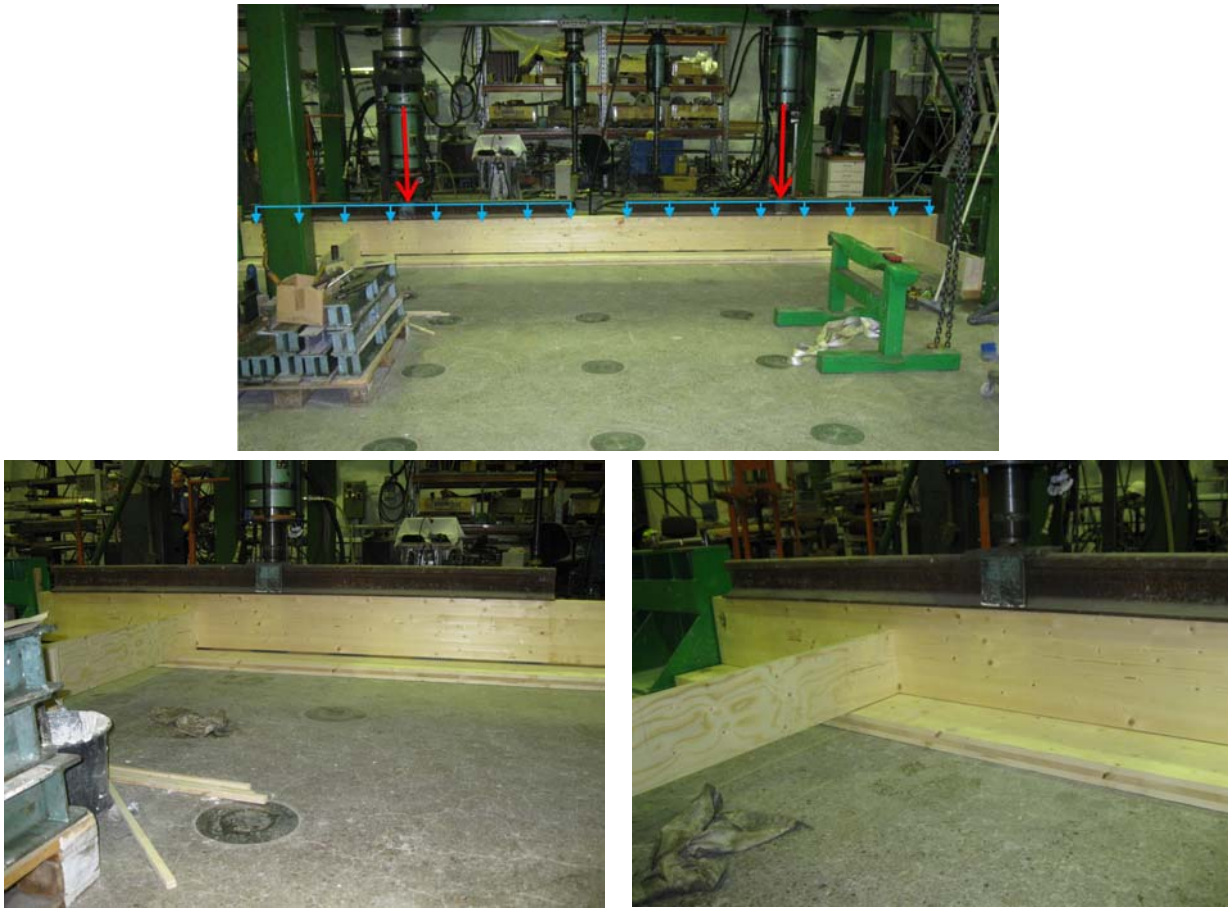

Fig. 9: Pressing of the glulam beam onto the DSNP preinstalled in the CLT with distributing steel beams.

Some double-sided nail plates were not fully pressed towards the ends of the two distributing steel beams. An additional pressing was done at the end of the beam until full contact was achieved. The pressing depth of the double-sided nail plate teeth was satisfactory with an average gap of less than 2 mm between the members. The nails of the nail plates become visible when the gap between the glulam and CLT elements exceeds 2.5 mm, see Fig. 10-a and Fig. 10-b. A remaining gap (about 3 mm) was observed at some locations for most of the specimens after the assembly was finished, usually at the second and third double-sided nail plate from the beam ends, and at the two ones at mid span.

(a) (b)

Fig. 10: Difference of pressing depth of the nail plates at different locations in the same beam: (a) Double-sided nail plate fully pressed (gap < 2.5 mm); (b) Double-sided nail plate with gap on the glulam side (gap ≥ 2.5 mm).

The inclined self-drilling screws of the test specimens B1_S and B3_NP+S were inserted some hours before carrying out the tests with a specific tool to control the 45° degree angle (Fig. 11).

Fig. 11: Assembly of the composite beam elements with inclined screws at 45°.

The assembly of the specimen with screw-gluing was done in the climate controlled room under 65% relative humidity and 20°C temperature. The glue opening time was 18 minutes, and the specimen cured for 24 hours before testing.

Figure 12: Assembly of the screw-glued beam in the climate controlled room.

2.6 Test setup

The bending tests were carried out under a four-points loading test arrangement. The composite beam lied on two poined supports with one having the possibility to slide horizontally. The support length was 100 mm on each side and represented the actual support conditions of a floor element on a CLT wall. The beam was supported over the entire CLT element width. The concentrated loads were positioned at the third points of the beam span of 6.4 m and distributed to the top of the glulam beam via two thick steel plates (250 mm × 90mm).

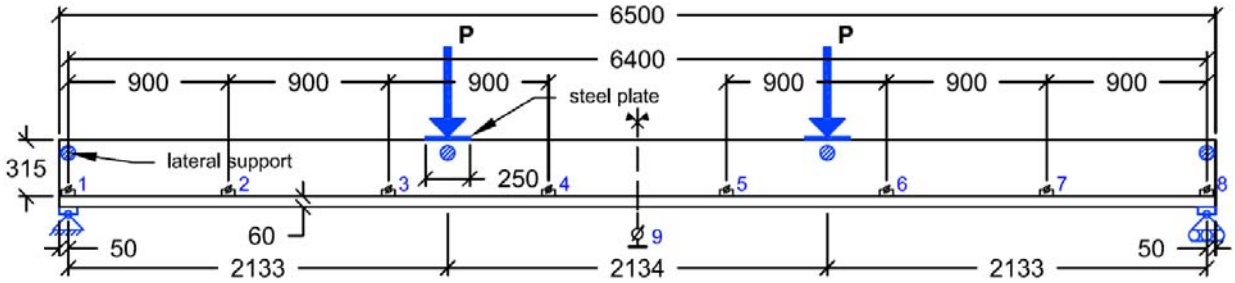

Fig. 13: Bending test setup (#1 to #8: LVDT longitudinal slip measurement; #9: mid-span global deflection measurement)

Fig. 14: View of the bending test setup

The global deflection at mid-span was measured from the bottom of the CLT panel with a Tokyo Sokki DP-500E inductive sensor. The longitudinal slip at the CLT-glulam interface was measured with linear displacement transducers (HBM-W10-TK) at each second shear connector positions along the beam from the beam ends (Fig. 13). The load was applied under load-control for the entire test with two VEB hydraulic jacks and measured by Instron UPM load cells, following the EN 26891 [15] loading procedure. The tests were stopped at the collapse of the beam.

Specific measurements for the deflection at mid-span δ and the slip v at certain load levels according to EN 26891 (cf. Fig. 15) are reported in Appendix C for each test specimen.

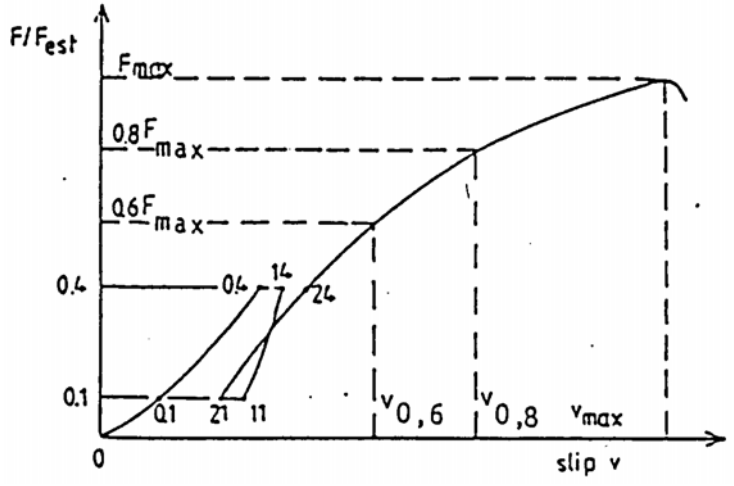

Fig. 15: Measurement points on a load-deformation curve according to EN 26891

2.7 Considered design load for the serviceability and ultimate limit states

The load levels corresponding to the serviceability limit state (SLS) for the characteristic load combination w_{SLS} and to the ultimate limit state (ULS) for the fundamental load combination w_{ULS} are defined from the uniformly distributed load case (G_k = 1.8 kN/m^2 and Q_k = 2 kN/m^2) for which the floor element is designed. The corresponding load levels considered in the 4-point bending test are noted, F_{SLS} and F_{ULS}, are obtained from the equivalence of the bending moment under the uniformly distributed loading and 4-point loading cases, with $F = 2 \cdot P = (3 \cdot w \cdot L)/4$, where F is the total load applied, P is a single point load (Fig. 13), w is the distributed load case and L is the span of the beam. Therefore, the load levels considered for the floor reduced cross-section of 580 mm width in the SLS and ULS are F_{SLS} = 10.6 kN and F_{ULS} = 14.1 kN, respectively. These values are used to evaluate the bending stiffness and performance of the shear connections from a practical point of view.

3 Experimental results

3.1 General

The load-deflection curves for all tests specimens tested are presented in Fig. 16. The collapse of the specimen is indicated by a marker at the end of each curve representing the end of the test. The design load levels considered F_{SLS} and F_{ULS}, defined in section 2.7, are also represented in Fig. 16.

The dashed lines represent the theoretical load-deflection calculated according to the γ-method (cf. section 2.3.1) using the measured global modulus of elasticity for each timber member (cf. section 2.2) and the slip modulus values from Table 1 and calculated with Eq. (18).

$$\delta = \frac{Fa\left(3L^2 - 4a^2\right)}{48EI} \tag{18}$$

The bending stiffness values used $EI_{ef,sls,calc}$ are given in Table 4. In beam configurations with combined shear connectors (DSNP and screws) the slip moduli of the different fastener types are added as suggested in [1]. For the screw-glued shear connections, full composite action between glulam and CLT is assumed. The flexibility due to the cross layer in the CLT panel remains considered in all cases.

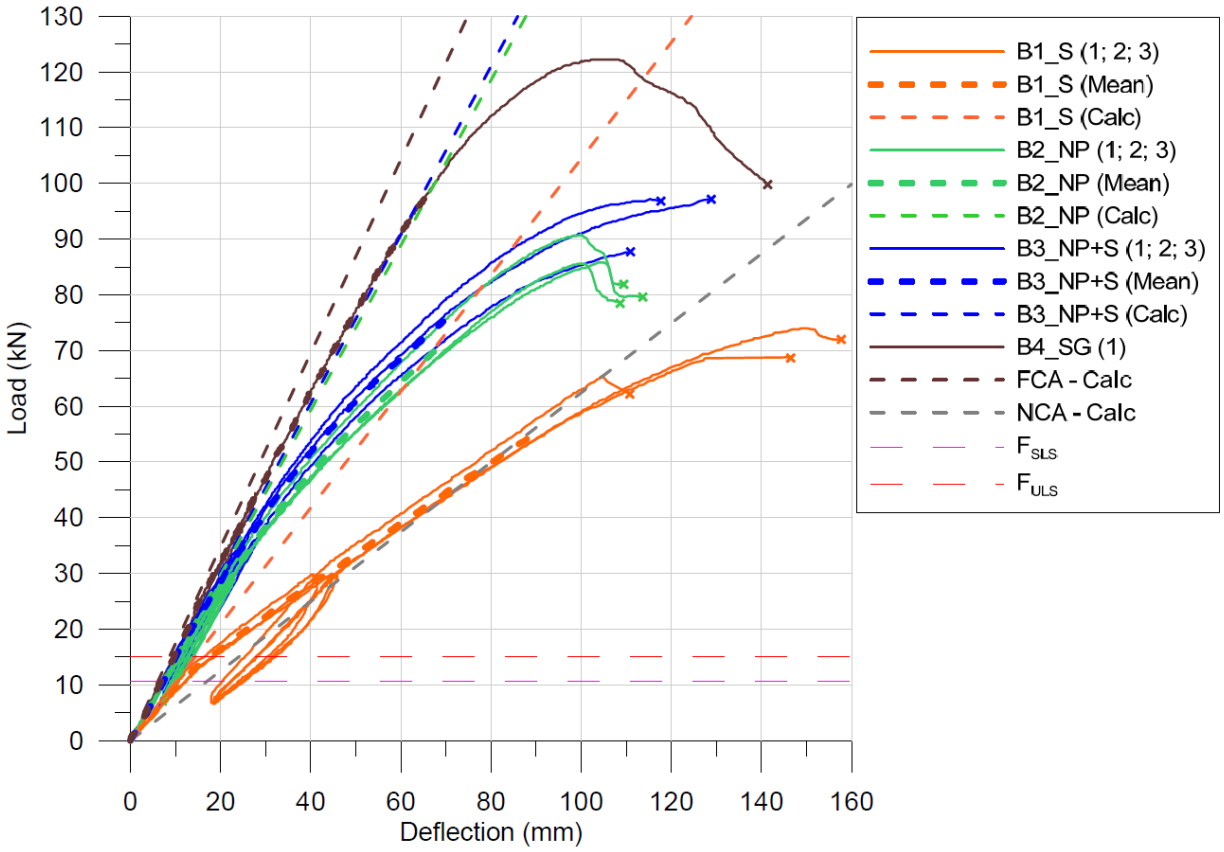

Fig. 16: Load-deflection curves for the four-point bending tests and calculated theoretical load-deflections

In Fig. 17, average load-deflection curves are presented up to 80% of the average maximum load of each test series.

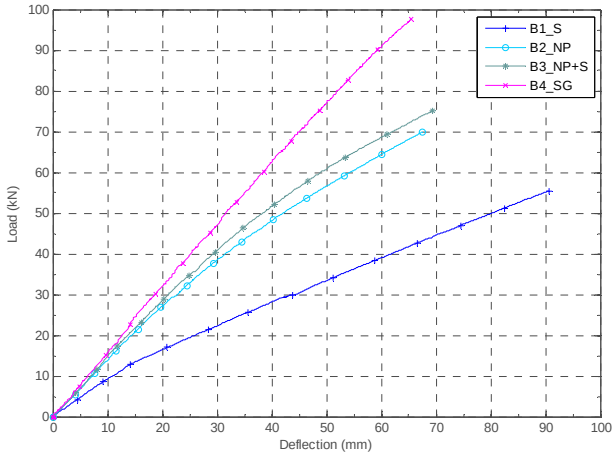

Fig. 17: Mean load-deflection curves for series B1_S, B2_NP and B3_NP+S, and single curve for B4_SG up to 80% of F_{max} for the test series (mean value)

The main results for each test series (mean values) are presented in Table 3 with the mean density $\rho_{g,\omega}$ and $\rho_{c,\omega}$ of the glulam and CLT members at the time of testing, respectively, the moisture content ω measured just after the bending tests, the maximum load F_{max}, the bending stiffness $EI_{04.Fmax}$ estimated between 10 % and 40 % of the observed maximum load F_{max}, the bending stiffness $EI_{F.SLS}$ estimated between the load levels F_{SLS} and $F_{SLS}/4$, the deflection at mid-span δ_{SLS} at the load F_{SLS}, and the ratio L/δ_{SLS} where L is the span of the beam element.

Table 3: Summary of the bending test results for the series with screws only (B1_S), nail plates only (B2_NP), nail plates and screws combined (B3_NP+S), and screw gluing (B4_SG) – Mean values.

Test series	No. of tests	Glulam		CLT		Maximum load	Failure load	Mid-span deflection at $0.4 \cdot F_{max}$	Span to deflection ratio at $0.4 \cdot F_{max}$	Mid-span deflection at F_{SLS}	Span to deflection ratio at F_{SLS}
		D	MC	D	MC						
		$\rho_{g,\omega}$ kg/m^3	ω_g (%)	$\rho_{c,\omega}$ kg/m^3	ω_c (%)	F_{max} (CoV) kN (%)	F_f (CoV) kN (%)	$\delta_{04 \cdot Fmax}$ (CoV) mm (%)	$L/\delta_{04 \cdot Fmax}$	δ_{SLS} (CoV) mm (%)	L/δ_{SLS}
B1_S	3	474	13.7	455	12.9	69.4 (6.2)	67.7 (7.4)	39.9 (12.8)	160	11.7 (7.4)	545
B2_NP	3	438	13.9	461	13.0	87.4 (3.4)	80.1 (2.0)	26.8 (0.7)	239	7.58 (3.5)	844
B3_NP+S	3	454	14.0	463	12.9	94.0 (5.9)	93.9 (5.8)	27.2 (2.2)	235	7.39 (4.0)	866
B4_SG	1	489	14.2	467	12.7	122	99.8	30.9	207	6.75	948

D = density, MC = Moisture Content

3.2 Failure observations

The test specimens with mechanical fasteners shear connection (series B1_S, B2_NP and B3_NP+S) failed by a tensile bending failure of the glulam beams starting from a finger joint or a knot in most of the cases. No visible damage could be observed in the CLT panels. Compression failure could be observed on the upper side of the glulam member between the points of load application for all test series, often down to the second glulam lamella.

The ultimate failure occurred in B1_S in the glulam member, triggering the sudden withdrawal some screws (both pull-through and pull out was observed). The timber members were tightly connected before failure. In series B2_NP the ultimate failure occurred in the glulam member. Before the glulam beam failure, the withdrawal of the DSNP could be observed and is characterised by a slight reduction of the load in Fig. 23 before failure. In series B3_NP+S, the inclined screws seem to have prevented the separation before the failure of the glulam beam, providing a slightly higher maximum load to the composite beam.

3.2.1 Series B1_S (Inclined screws only)

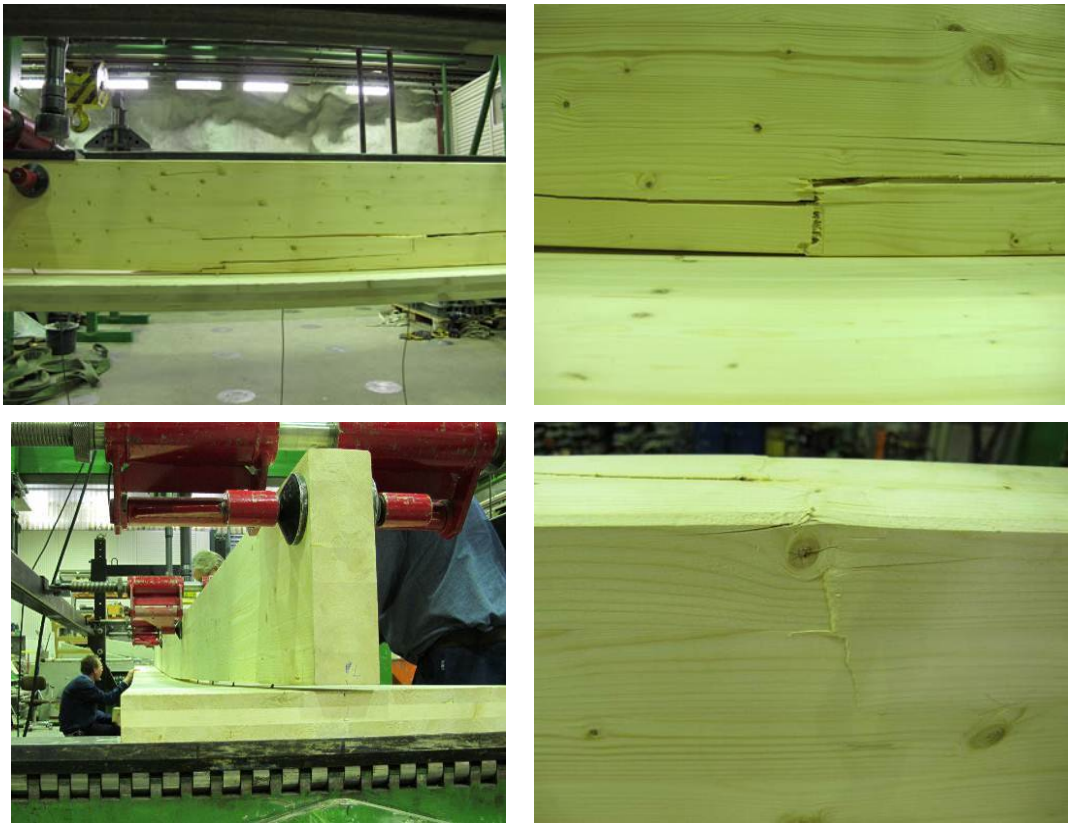

Fig. 18: Pictures of beam specimens after failure (Series B1_S)

3.2.2 Series B2_NP (Double-sided nail plates only)

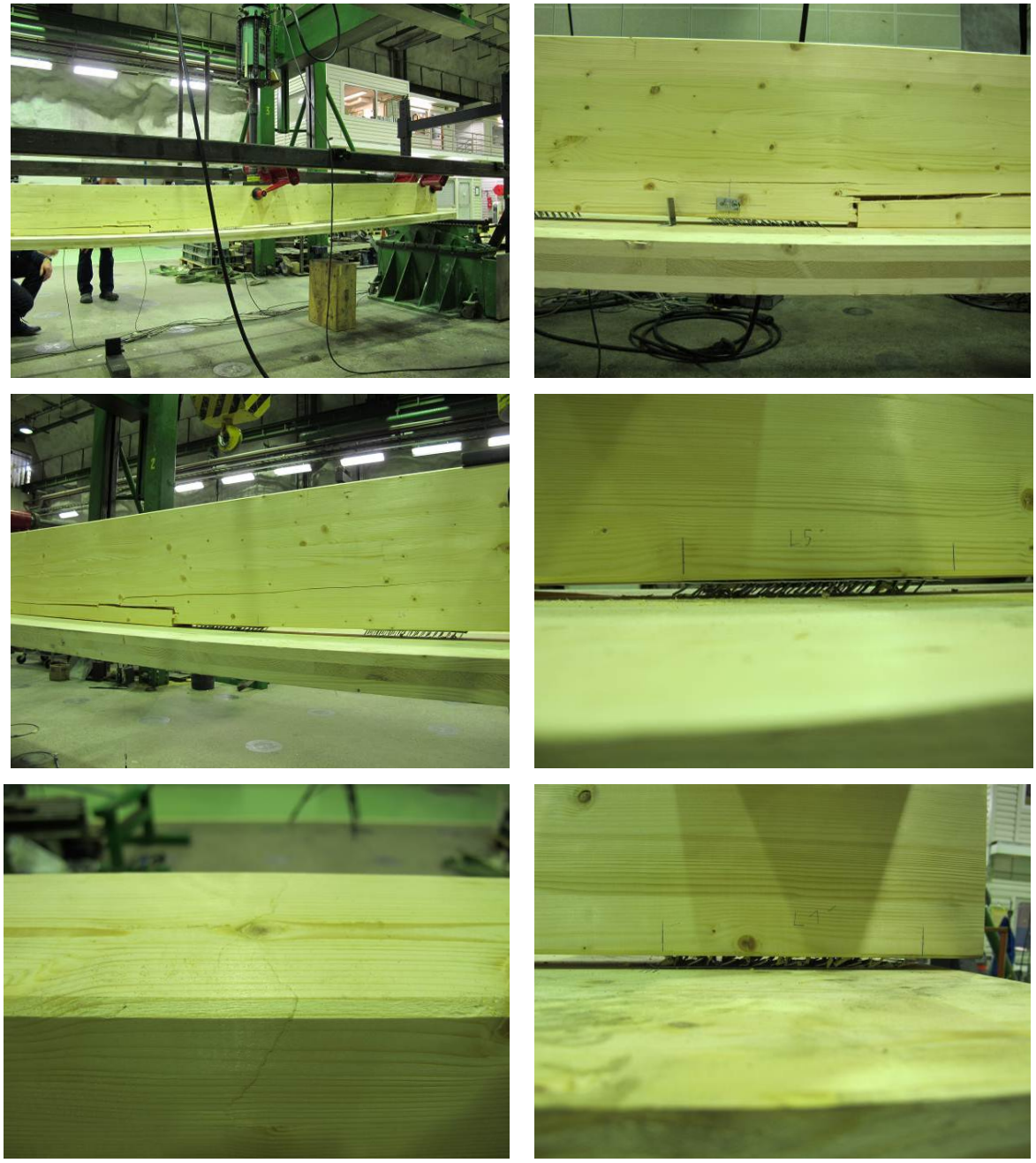

Fig. 19: Pictures of beam specimens after failure (Series B2_NP)

3.2.3 Series B3_NP+S (Double-sided nail plates and inclined screws combined)

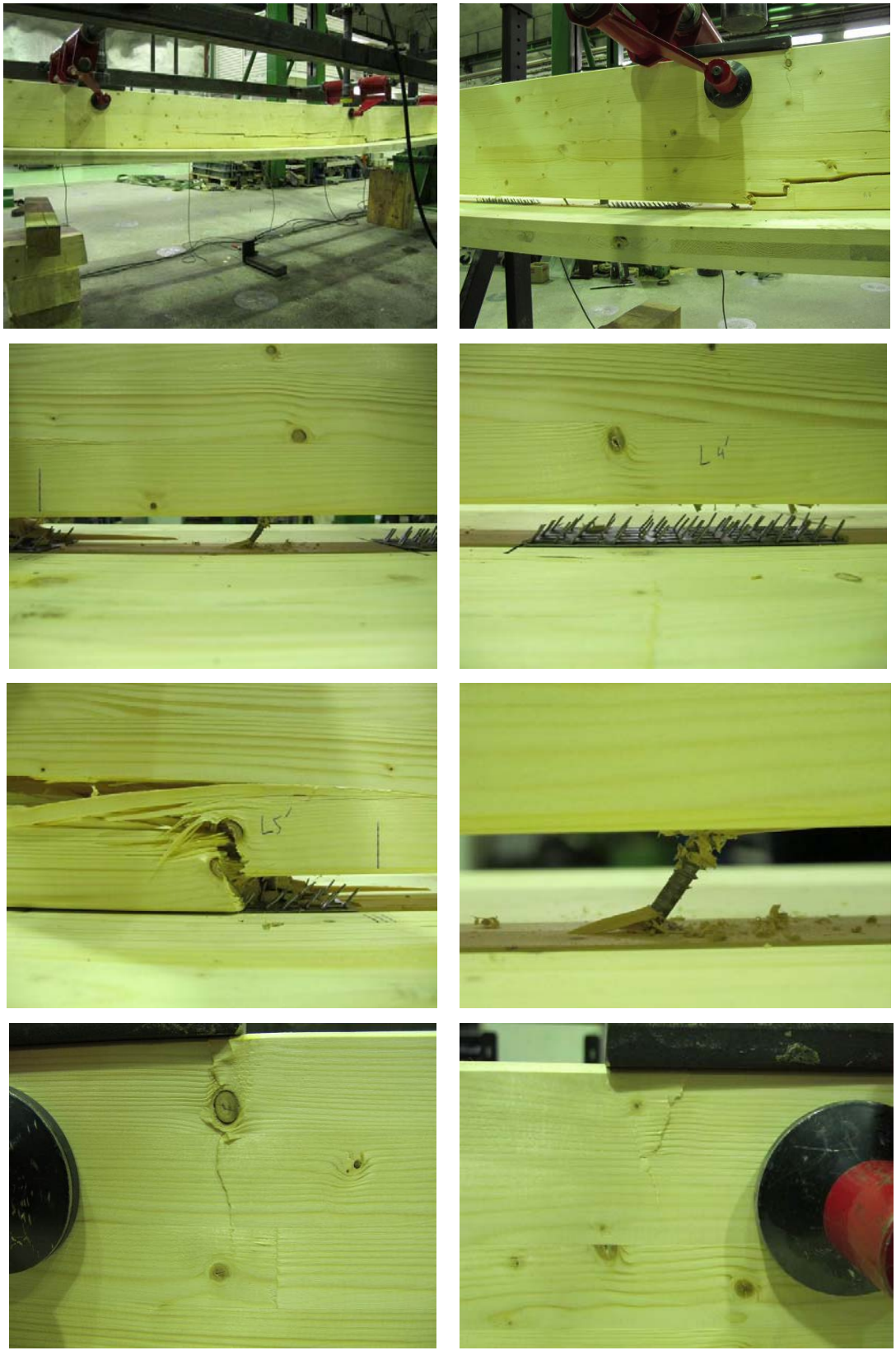

Fig. 20: Pictures of beam specimens after failure (Series B3_NP+S)

3.2.4 Series B4_SG (Screw-gluing)

For the specimen B4_SG, a tensile bending failure in the CLT panel (Fig. 21 (b) and (d)) and a very large compression failure at the top of the glulam beam were observed (Fig. 21 (b) and (c)). The compression failure, located near the load application point, extended down to half the height of the glulam beam, and could be observed before the CLT panel failure (Fig. 21 (a)). The glue line at the glulam-CLT interface did not fail and no separation of the members was observed.

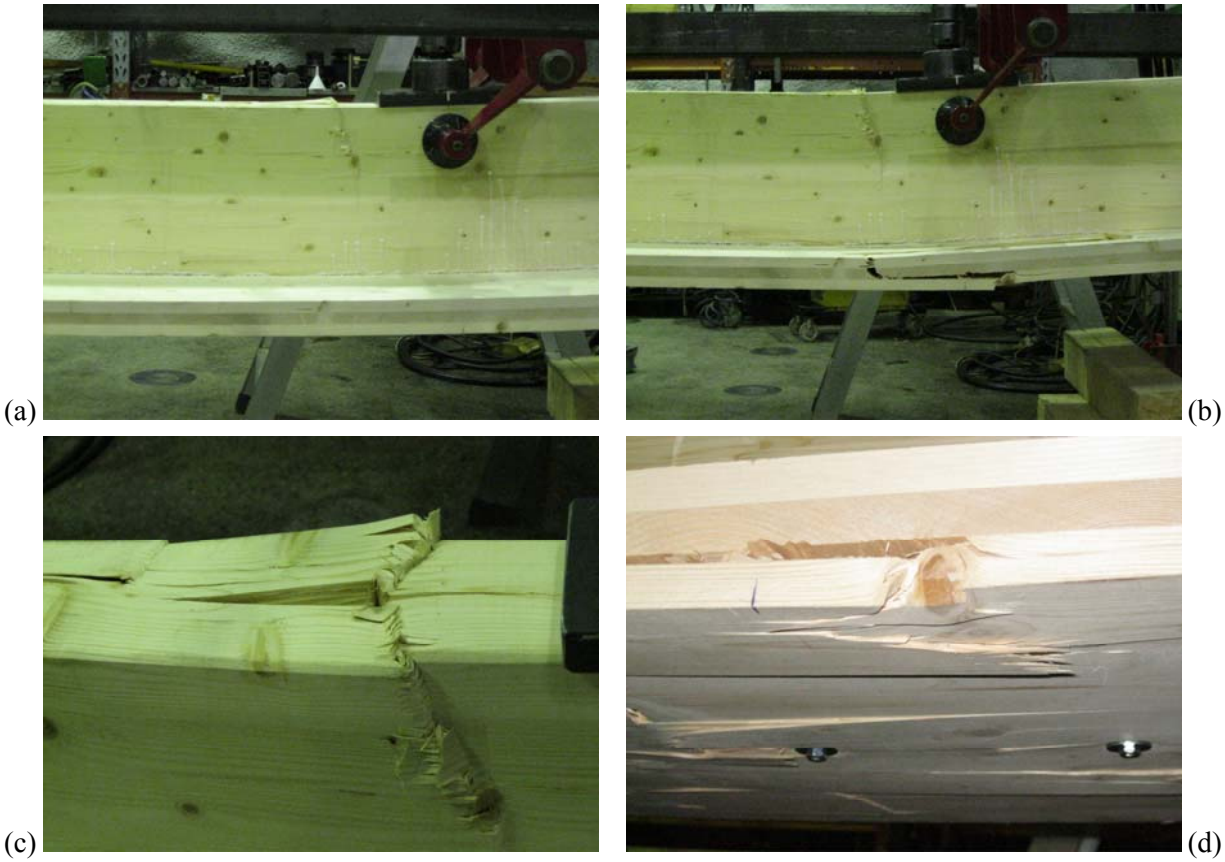

Fig. 21: Failure observations series B4_SG: (a) large compression failure of the glulam beam before collapse, (b) compression failure of the glulam and tension failure of the CLT, (c) compression failure of the glulam, (d) tensile bending failure of the CLT.

3.3 Load-deflection curves – individual test series.

The load-deflection curves at mid-span are presented in Fig. 22 to Fig. 25 for each test series with a closer view up to about 50% of the estimated failure load F_{est}. The individual load-deflection curves and load-slip measurements along the beam are presented for each test specimen individually in Appendix B with more detailed tables of results, Appendix C.

In Fig. 22 (Series B1_S), a change in the slope at about 13 kN can be observed, indicating a change in the shear connection behaviour. A clear sound of static friction being exceeded at regular time intervals (about 1 s) and causing regular slip increments could be heard along the tests, starting at about 10 kN.

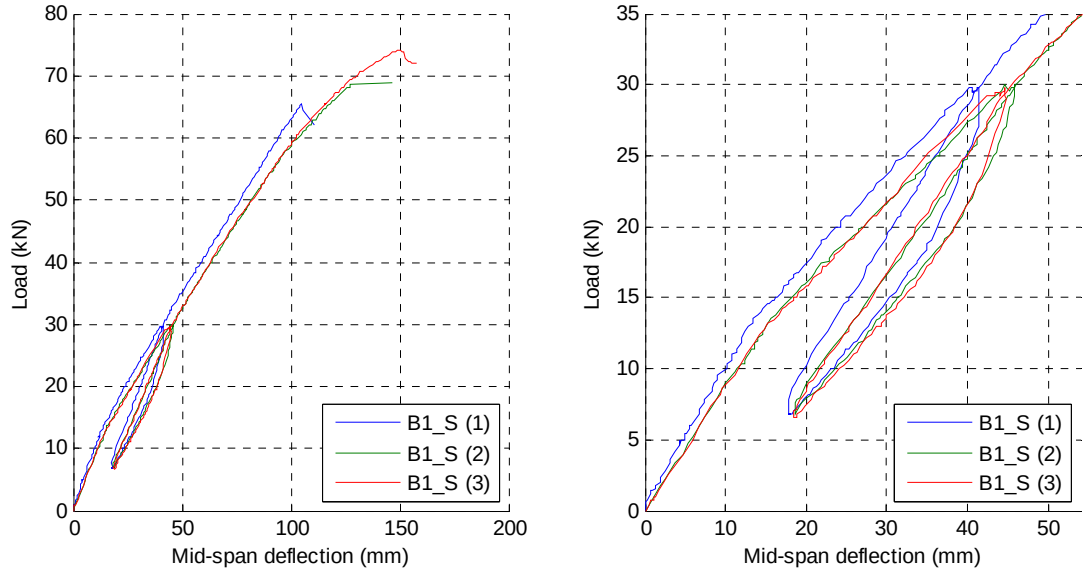

Fig. 22: Load-deflection curves at mid-span (full curves and curves up to 50% of F_{est}) - Series B1_S

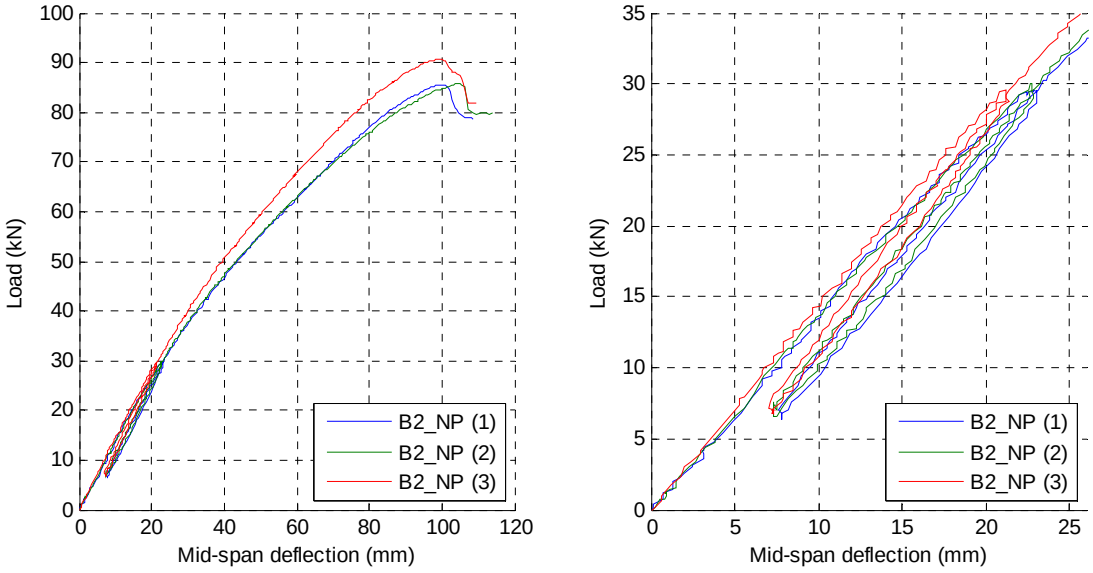

Fig. 23: Load-deflection curves at mid-span (full curves and curves up to 50% of F_{est}) - Series B2_NP

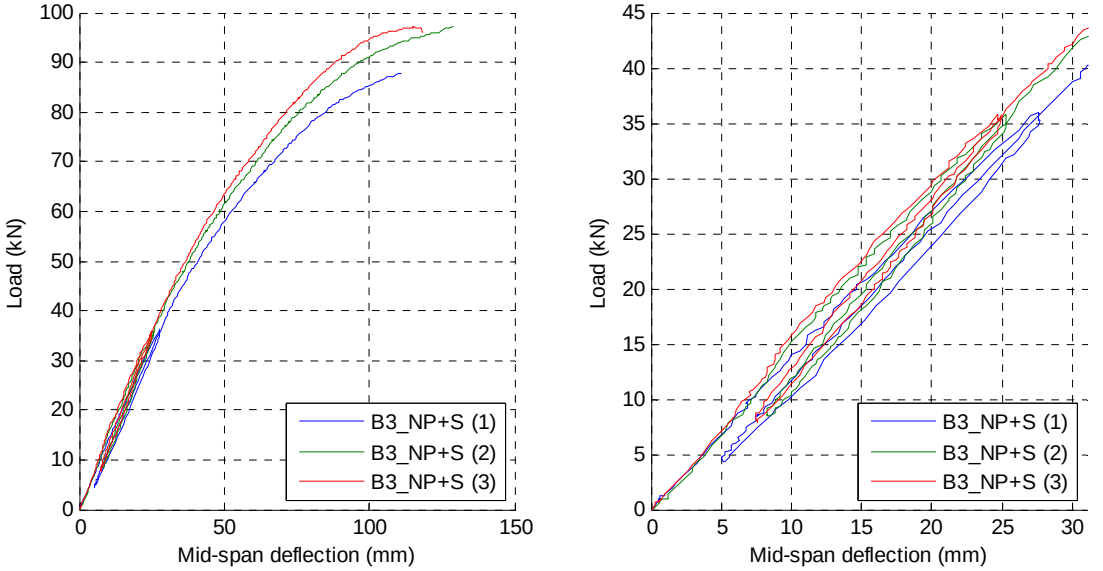

Fig. 24: Load-deflection curves at mid-span (full curves and curves up to 50% of F_{est}) - Series B3_NP+S

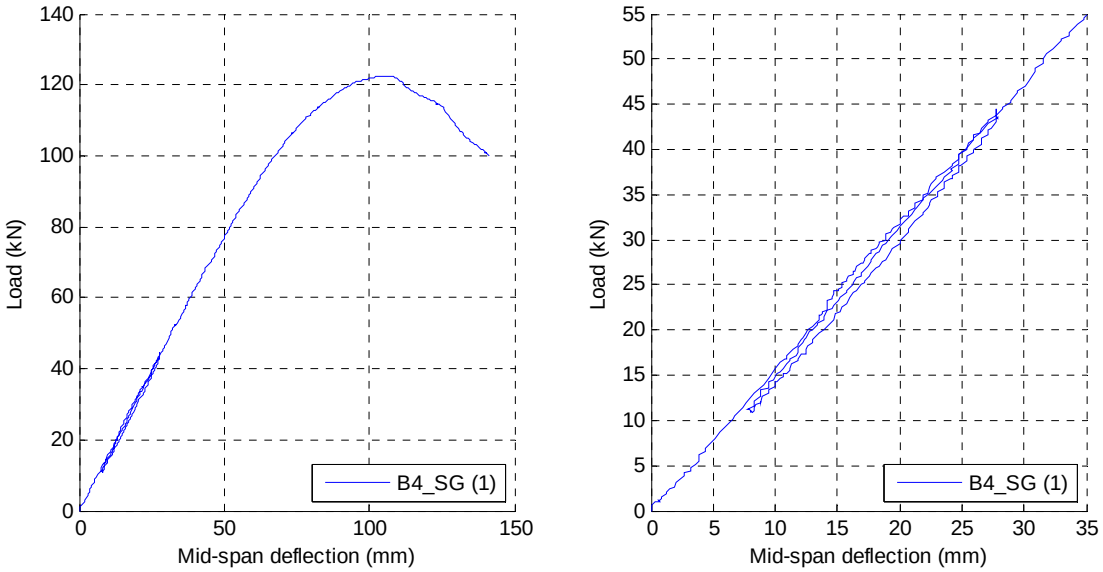

Fig. 25: Load-deflection curves at mid-span (full curves and curves up to 50% of F_{est}) - Series B4_SG

3.4 Slip measurements along the beam length - individual test series.

The measured slip v at the glulam-CLT interface is plotted in Fig. 26 to Fig. 28 along the beam length for the test series B1_S, B2_NP and B3_NP+S at certain load values F_{01}, F_{04}, F_{06}, F_{08}, F_{max}, and $F_{failure,}$ ($F_{failure}$ being the last load level recorded before a drop of load of more than 20 %). For the series B4_SG the slip was only measured at both beam ends and is presented in the result tables in Appendix C.

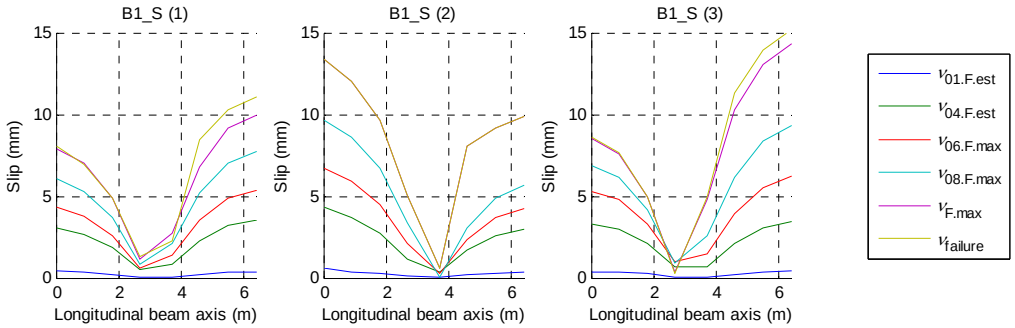

Fig. 26: Slip measurements along the beam length at the load levels F_{01}, F_{04}, F_{06}, F_{08}, F_{max}, and $F_{failure}$ – Series B1_S

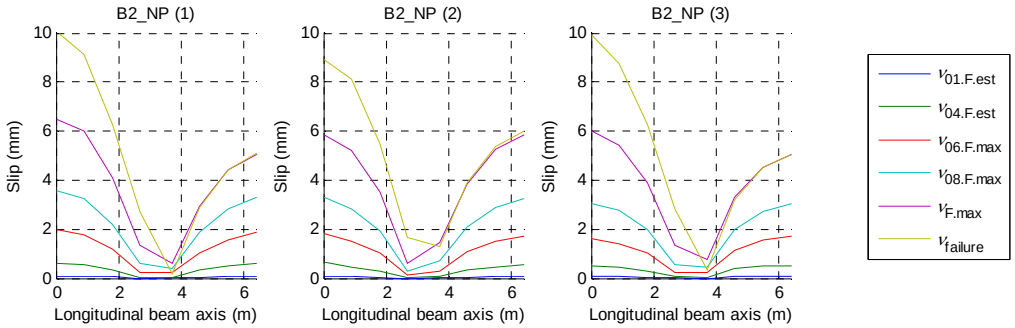

Fig. 27: Slip measurements along the beam length at the load levels F_{01}, F_{04}, F_{06}, F_{08}, F_{max}, and $F_{failure}$ – Series B2_NP

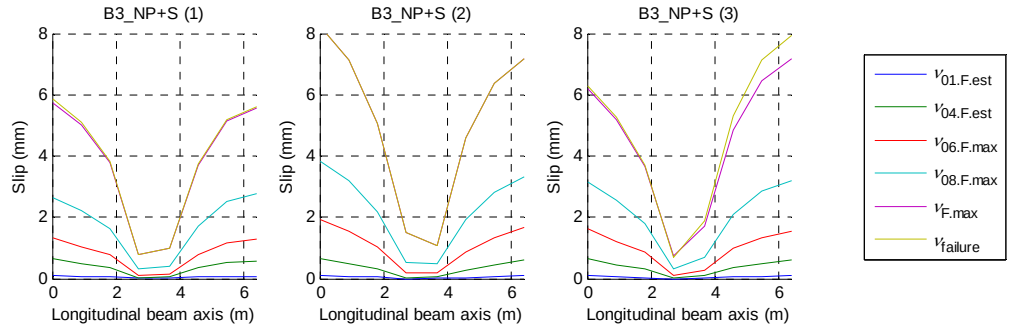

Fig. 28: Slip measurements along the beam length at the load levels F_{01}, F_{04}, F_{06}, F_{08}, F_{max}, and $F_{failure}$ – Series B3_NP+S

3.5 Bending stiffness of the composite beams

In Table 4, the bending stiffness is evaluated between different load levels, between 10 % and 40 % of F_{max} for each test specimen, and between F_{SLS} /4 and F_{SLS}, load levels which are the same in all test series. The calculated bending stiffnesses $EI_{ef,sls,calc}$ are the values used for plotting the theoretical load-deflections in Fig. 16. The corresponding degree of composite action DCA for each series is calculated according to Eq. (19):

$$\mathrm{DCA} = \frac{EI_{ef} - EI_0}{EI_\infty - EI_0} \times 100 \tag{19}$$

where EI_{ef}, EI_0 and EI_∞ are the effective bending stiffness of the partially composite section, the bending stiffness of the non-composite section, and the bending stiffness of the fully composite section, respectively. Concerning the bending stiffness estimated based on the load-deflection curves between $F_{SLS}/4$ and F_{SLS}, the degree of composite action is calculated for two cases, the first with EI_∞ calculated considering full composite action between the glulam and CLT, and the second considering the estimated value of the bending stiffness in series B4_SG.

Table 4: Calculated bending stiffness of the floor element and degree of composite action (DCA) of the composite section

Test series	Bending stiffness between $0.1 \cdot F_{max}$ and $0.4 \cdot F_{max}$	Bending stiffness between $F_{SLS}/4$ and F_{SLS}			Bending stiffness calculated based on measured MOE and connectors serviceability slip modulus	
	$EI_{04 \cdot Fmax}$ MN·m^2	$EI_{F.sls}$ MN·m^2	DCA with $EI_{F.sls}$ and EI_∞ ~ FCA (%)	DCA with $EI_{F.sls}$ and EI_∞ ~ EI_{B4_SG} (%)	$EI_{ef,sls,calc}$ MN·m^2	DCA with $EI_{ef,sls,calc}$ (%)
*NCA (EI_0)					2.90	0
B1_S	3.00	4.13	23.7	26.0	4.86	37.7
B2_NP	5.99	6.57	70.9	77.6	6.89	77.0
B3_NP+S	6.35	6.96	78.3	85.8	7.04	79.9
B4_SG	7.40	7.63	91.3	100	8.08	100
**FCA (EI_∞)					8.08	100

*NCA = No composite action ($EI_{ef,sls,calc} = EI_0$ is the sum of the bending stiffness of the glulam beam and the CLT panel)

**FCA = Full composite action ($EI_{ef,sls,calc} = EI_\infty$ is calculated assuming that no slip can occur between the glulam and the CLT)

The bending stiffness estimated in series B1_S is low due to low level of composite action provided by the screw shear connection in this configuration. $EI_{04 \cdot Fmax}$ is very close to the bending stiffness of the non-composite section (NCA) for series B1_S while $EI_{F.sls}$ is closer to the theoretical value. This is due to the early non-linear response of the beam specimens in this test series caused by the weak shear connection used.

The bending stiffnesses in series B2_NP and B3_NP+S are high due to the high slip modulus of the double-sided nail plate shear connection. A difference of about 10% between $EI_{04\cdot Fmax}$ and $EI_{F.sls}$ can be noted for both test series. The addition of inclined screws slightly increases the bending stiffness at the both load levels considered in Table 4. The level of composite action with DSNP is high and the bending stiffness values obtained are relatively close to the one of the screw-glued test specimen.

The screw-glued specimen did exhibit a high level of composite action but some slip nevertheless occurred between the CLT and glulam members, explaining part of the mismatch between the calculated theoretical values of the bending stiffness considering full composite action (FCA) and the estimation from tests. The values $EI_{F.sls}$ and $EI_{ef,sls,calc}$ are very compared to the other test series. This composite beam behaves more linearly with respect to its load-carrying capacity than the beams in the other test series.

3.6 Estimation of the floor element fundamental frequency

The governing design criterion for the floor structure evaluated in this study is the minimum requirement specified by the Finnish National Annex for the vibration in the serviceability limit state. The fundamental frequency of the finished floor structure for the design case considered in this study (G_k = 1.8 kN/m^2) is calculated for each test series according to Eq. (13) and presented in Table 5. In addition the corresponding maximum span fulfilling the 9 Hz criterion is calculated using either the estimated bending stiffness $EI_{F.sls}$, or $EI_{ef,sls,calc}$ (cf. Table 4). The δ_{1kN} is not calculated here as the result largely depends on the stiffness of the complementing layers increasing the bending stiffens in the transverse direction. An example is given in Appendix A.

Table 5: Calculated fundamental frequency of the finished floor (6.4 m span) based on the bending stiffness estimated from tests and predicted by calculation, $f_{1,F.sls}$ and $f_{1,ef,calc}$ respectively, and maximum span fulfilling the 9 Hz limit criteria.

Test series	$f_{1,F.sls}$ (using $EI_{F.sls}$)	Max. span for $f_{1,F.sls} \geq 9$ Hz	$f_{1,ef,calc}$ (using $EI_{ef,sls,calc}$)	Max. span for $f_{1,ef,calc} \geq 9$ Hz
	(Hz)	(m)	(Hz)	(m)
NCA (EI_0)			5.87	5.17
B1_S	7.00	5.64	7.60	5.88
B2_NP	8.83	6.34	9.05	6.42
B3_NP+S	9.09	6.43	9.14	6.45
B4_SG	9.52	6.58	9.80	6.68
FCA (EI_∞)			9.80	6.68

According to the test results, only the series B3_NP+S and B4_SG satisfy the 9 Hz limit criteria. Considering the calculated values, series B2_NP is also fulfilling the vibration criteria for 6.4 m span. The low modulus of elasticity of the glulam beams measured in this study compared to the values to be expected according to the material strength class can explain the relatively low fundamental frequency calculated compared to the values obtained in the design example (cf. Appendix A) where the moduli of elasticity given in [5] and [16] are considered.

3.7 Longitudinal slip at the glulam-CLT interface

The longitudinal slip values along the glulam-CLT interface, $v_{F.sls}$, $v_{F.uls}$ and $v_{04.Fmax}$ for the load levels F_{sls}, F_{uls} and $F_{04.Fmax}$, respectively, are shown in Fig. 29 for each test specimen and compared to the yield slip values observed in the shear tests for the screws and double-sided nail plates [1] (cf. Table 1). The slip at $0.4 \times F_{max}$ exceeds for all series the yield slip of the double-sided nail plates since the design of the beams is governed by the shear connection strength and stiffness and that the beam load-carrying capacity exceeds the design loads. As a practical evaluation the observations of the slip can be made at the design load levels F_{SLS} and F_{ULS} defined in section 2.7. The theoretical slip value at the end of the beam at the SLS and ULS calculated using Eq. (9) and the individual slip modulus of a single fastener is also shown with markers in Fig. 29, and noted $v_{sls,2P,calc}$ and $v_{uls,2P,calc}$.

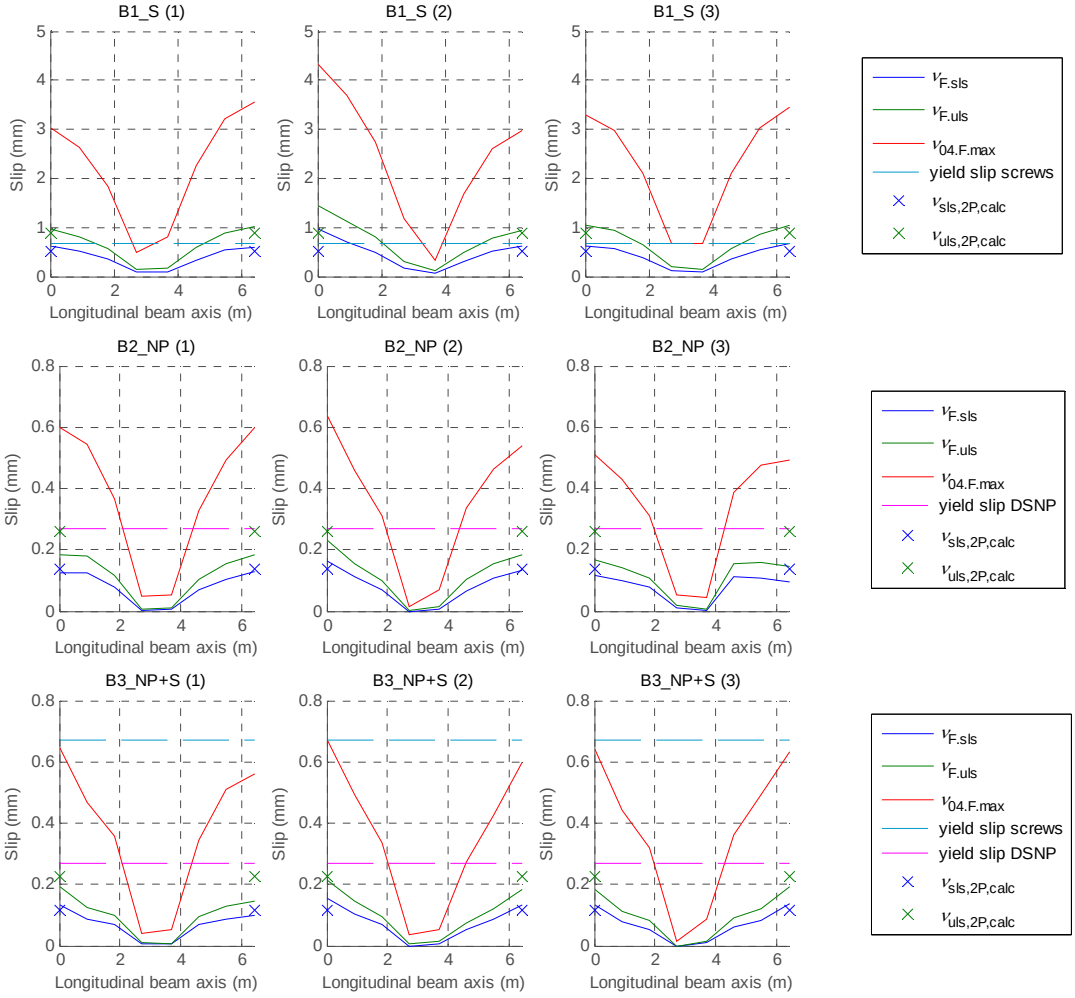

Fig. 29: Interface slip along the beam axis at load level F_{SLS}, F_{ULS}, $F_{04\cdot Fmax}$, yield slip values for the connectors used.

The longitudinal slip in series B4_SG was measured at both ends only. At F_{sls}, the end slip measured on each side was 0.031 mm and 0.006 mm, and at F_{uls}, the slip was 0.045 mm and 0.016 mm one each side. We note however a significant difference between the two end-slip measurements, indicating a possible defect of the screw-gluing joint on one side.

4 Discussion

4.1 Combination of inclined screws and double-sided nail plates

One of the aims of this study was to assess the technical feasibility of a glulam-CLT composite beam connected with double-sided punched metal plate fasteners. It was also considered necessary to compare the behaviour of the double-sided nail plates used alone or in combination with inclined screws in order to evaluate if a possible premature failure of the double-sided nail plate joint could be prevented with inclined screws. The results show that with the present design, double-sided nail plates performed well in a static loading situation and that the addition of inclined screws provides a limited advantage in terms of stiffness and behaviour near failure load. It should be noted that the long term performance of the joint has not been evaluated and that for this purpose, the presence of the screws might still be beneficial.

It was noted in [1] that the inclined screws and the double-sided nail plates had different load-displacement responses. It was mentioned that the slip moduli of the different fasteners could be added in this specific combination but that the combination was not optimal in terms of load-carrying capacity of the fasteners. It was argued that a different inclination angle, about 30° instead of 45° could be used to obtain a better compatibility with the double-sided nail plates in terms of load-carrying capacity, noting that a lower angle would reduce the stiffness contribution of the screws in the joint. Since the behaviour of DSNP shear connectors is satisfactory in the bending test situation and that a rather high level of composite action can be reached with DSNP only, the use of vertical screws to only secure the connection for handling purpose (floor element manufacturing and on-site assembly) and safety in case of major damage of the floor element could also be considered as an alternative.

4.2 Floor element layout and failure

The fact that the CLT panel is located at the bottom of the composite beam is advantageous for the failure of the beam (Fig. 2). The large CLT bottom flange limits the tensile stresses in the glulam beam and provides the possibility for a more ductile failure with the development of a compression failure at the top of the beam prior to the tensile bending failure.

4.3 Design and buildability considerations

The design example (cf. Appendix A) shows that the long-term performance is not a decisive design criterion for this composite beam design with double-sided nail plates. Concerning the design of a residential building according the Eurocode 5 and Finnish National Annex, the vibration requirement in the SLS is the primary governing design criteria, far from the long-term strength and static instantaneous deflection limits in the SLS. The bending stiffness and therefore the stiffness of the shear connection are crucial parameters for the design of the floor elements when other design levers are fixed (floor height, effective glulam beam width, etc.) which is often the case in multi-storey residential construction.

The relevance (viability, cost efficiency) of a glulam-CLT floor solution with double-sided nail plates depends on the manufacturing possibilities. The assembly of the beam elements performed in the laboratory show that it is technically feasible to connect long timber members together by pressing simultaneously a number of double-sided nail plates. With equipment specifically designed for the assembly of such elements, it should be possible to create a cost efficient solution for glulam CLT composite floors connected with double-sided nail plates, with possibly a high level of automation. The results also showed that it is possible to reach a high level of composite action with this type of shear connector and that it is suitable for medium span floor elements.

5 Conclusions

The double-sided nail plates showed an appropriate behaviour as a shear connector in the bending tests. No early separation of the timber members due to a lack of withdrawal capacity of the nail plates was observed. Concerning the failures observed the separation in series B2_NP actually occurs at a very high load level suggesting that double-sided nail plates may even be used without screws or with a more limited amount of them. It should be noted that some further verifications might be necessary concerning the double-sided nail plates behaviour under repeated loadings, long-terms loading situations and behaviour in case of fire.

The present design of the beam is governed by the shear connection stiffness due to the vibration requirements in the SLS. Calculations of bending stiffness using the γ-method agree reasonably well with the test results considering the input values (slip modulus) from previous shear tests on these connectors.

The level of composite action achieved between the glulam beam and the CLT panel is relatively high with shear connections made with double-sided nail plates. The influence of the inclined screws is considered small when combined to double-sided nail plates. In the combined joint, a small and predictable increase of the strength and bending stiffness could be observed as well as a slightly different behaviour near failure load, the screws seeming to prevent the withdrawal of the nail plates before collapse of the beams.

Appendix A: Design of a glulam-CLT element according to Eurocode 5 and Finnish National Annex

The design procedure for a glulam-CLT floor element connected with double-sided punched metal plate fasteners according to Eurocode 5 and Finnish National Annex is presented here. The design concerns the simply supported beam element presented in Fig. 2 for a span L = 6.4 m under a uniformly distributed loading. The design verifications cover the ultimate limit state for the short-term (A.2.1) and long term (A.2.2), and the serviceability limit state short term (A.2.3) and long term (A.2.4). A table summarises the results of the design procedure at the end of this Appendix.

A.1 Design data:

The material partial safety factor are γ_M = 1.25 for the CLT and punched metal plate fasteners, and γ_M = 1.20 for the glulam. The modification factors for service classes and load duration classes are k_{mod} = 0.8 (medium term action), k_{def} = 0.6 (timber members in service class 1 and permanent actions) for the timber members, and $k_{def,f} = 2 \cdot k_{def}$ = 1.2 (fasteners in service class 1 and permanent actions) for the fasteners. The ψ factors for residential buildings are ψ_0 = 0.7, ψ_1 = 0.5, and ψ_2 = 0.3.

The permanent load (self-weight and finishes) considered is G_k = 1.80 kN/m^2 and the imposed load (medium term) is Q_k = 2.00 kN/m^2.

A.1.1 Element 1: glulam beam GL32

Dimensions: h_1 = 315 mm and b_1 = 90 mm.

Modulus of elasticity: E_1 = 13.7 GPa (mean modulus of elasticity parallel)

$E_{1,fin} = E_1/(1+k_{def})$ = 8.56 GPa (long-term mean modulus of elasticity parallel).

Bending strength:

$f_{m,1,k}$ = 32 MPa (characteristic value)

$$f_{m,1,d} = \frac{k_{\text{mod}} \cdot k_h}{\gamma_M} f_{m,1,k} = 22.75 \text{ MPa}$$ (design value for medium term actions)

with k_h the factor accounting for the size effect of the glulam beam calculated $k_h = \min \begin{cases} (600/h_1)^{0.1} \\ 1.1 \end{cases}$

Tensile strength parallel:

$f_{t,0,1,k}$ = 22.5 MPa (characteristic value)

$f_{t,0,1,d} = \frac{k_{\mathrm{mod}} \cdot k_h}{\gamma_M} f_{t,0,1,k}$ = 16.00 MPa (design value for medium term actions)

Shear strength:

$f_{v,1,k}$ = 3.8 MPa (characteristic value)

$f_{v,1,d} = \frac{k_{\mathrm{mod}}}{\gamma_M} f_{v,1,k}$ = 2.53 MPa (design value for medium term actions)

A.1.2 Elements 2 and 3: CLT according to ETA-08/0271

h_2 = 20 mm (longitudinal layer height)

h_{23} = 20 mm (cross layer height)

h_3 = 20 mm (longitudinal layer height)

$b_2 = b_3 = b_{unit}$ = 580 mm (CLT layer width, beam element width)

$E_2 = E_3$ = 11.0 GPa (mean modulus of elasticity parallel)

E_{23} = 370 MPa (mean modulus of elasticity perpendicular)

$E_{2,fin} = E_{3,fin} = \frac{E_2}{1 + k_{def}}$ = 6.88 GPa (long-term mean modulus of elasticity parallel)

G_R = 50 MPa (mean rolling shear modulus)

$G_{R,fin} = \frac{G_R}{(1 + k_{def})}$ = 31.25 MPa (long-term mean rolling shear modulus)

Bending strength:

$f_{m,2,k} = f_{m,3,k} = k_l \cdot f_{m,C24,k}$ = 26.4 MPa

with k_l the system factor for CLT calculated as $k_l = \min \begin{cases} 1 + 0.025 \cdot n_l \\ 1.1 \end{cases}$ with n_l the number of adjacent single boards making the CLT layer according to [8].

$f_{m,2,d} = f_{m,3,d} = \frac{k_{\mathrm{mod}}}{\gamma_M} f_{m,2,k}$ = 16.90 MPa (design value for medium term actions)

Tensile strength parallel:

$f_{t,0,2,k} = f_{t,0,3,k}$ = 14 MPa

$f_{t,0,2,d} = f_{t,0,3,d} = \frac{k_{\mathrm{mod}}}{\gamma_M} f_{t,0,2,k}$ = 8.96 MPa (design value for medium term actions)

Rolling shear strength (for the verification of the cross layer):

$f_{R,k}$ = 1.25 MPa

$f_{R,d} = \frac{k_{\text{mod}}}{\gamma_M} f_{R,k}$ = 0.8 MPa (design value for medium term actions)

A.1.3 Shear connection: SE2P double-sided nail plates (200×72 mm²)

Fastener strength:

The single fastener characteristic strength value $F_{Rk} = (1 - 2.33 \cdot 0.032) \cdot F_{Rm}$ = 29.58 kN is calculated according to [17], where 2.33 is used to obtain the characteristic value under the 0.05 fractile for 6 test replicates with 75% confidence level, and F_{Rm} = 31.96 kN is the mean single fastener strength from the test series (S8_1NP-200) in [1], and 0.032 is the corresponding coefficient of variation.)

$F_{Rd} = \frac{k_{\text{mod}}}{\gamma_M} F_{Rk}$ = 18.93 kN (design single fastener strength for medium term actions)

Fastener slip modulus:

k_s = 53.6 kN/mm (single fastener SLS slip modulus) [1]

$k_u = \frac{2}{3} k_s$ (single fastener ULS slip modulus)

s = 450 mm (connectors spacing)

The corresponding smeared slip moduli are given by $K_{1,s} = \frac{k_s}{s}$ = 119.12 kN/mm/m, and $K_{1,u} = \frac{k_u}{s}$ = 79.41 kN/mm/m for the short-term SLS and ULS verification, respectively, and $K_{1,s,fin} = \frac{K_{1,s}}{(1 + k_{def,f})}$ = 54.14 kN/mm/m, and $K_{1,u,fin} = \frac{K_{1,u}}{(1 + k_{def,f})}$ = 36.10 kN/mm/m for the long-term SLS and ULS verifications, respectively.

A.2 Calculations under the different load combinations:

A.2.1 ULS short term:

Fundamental combination: $\gamma_G \cdot K_{FI} \cdot G_k + \gamma_Q \cdot K_{FI} \cdot Q_k$

with K_{FI} = 1.0 the safety factor for reliability class RC2 (residential building ≤ 8 storeys), and γ_G = 1.15 in Eq. (6.10b) of the Finnish National Annex to SFS EN-1990. Note that the load combination with permanent loads only (Eq. (6.10b)) is not considered in this example because it is evident that it is less demanding than Eq. (6.10b) for the load case considered, both for the short and long term verifications.

The load case for the single beam unit is given by w_{ULS}:

$$w_{ULS} = \left(\gamma_G \cdot K_{FI} \cdot G_k + \gamma_Q \cdot K_{FI} \cdot Q_k\right) \cdot b_{unit} = \left(1.15 \cdot 1.00 \cdot 1.80 + 1.5 \cdot 1.00 \cdot 2.00\right) \cdot 0.58 = 2.94 \text{ kN/m}$$

Design bending moment: $M_{ULS,d} = \left(w_{ULS} \cdot L^2\right)/8 = 15.06$ kN·m

Design shear force: $V_{ULS,d} = \left(w_{ULS} \cdot L\right)/2 = 9.41$ kN

Bending stiffness of the composite beam for the ULS verifications according to Eq. (1) to (6) in this report:

$$\gamma_{1,u} = \left(1 + \pi^2 \frac{E_1 A_1}{K_{1,u} L^2}\right)^{-1} = 0.459$$

$$\gamma_3 = \left(1 + \pi^2 \frac{E_3 A_3 h_{23}}{G_R b_3 L^2}\right)^{-1} = 0.979$$

$$a_{2,u} = \frac{\gamma_{1,u} E_1 A_1 \left(\frac{h_1 + h_2}{2}\right) - \gamma_3 E_3 A_3 \left(\frac{h_2 + h_3}{2} + h_{23}\right)}{\gamma_{1,u} E_1 A_1 + \gamma_2 E_2 A_2 + \gamma_3 E_3 A_3} = 57.71 \text{ mm}$$

$$a_{1,u} = \frac{h_1 + h_2}{2} - a_{2,u} = 109.79 \text{ mm}$$

$$a_{3,u} = \frac{h_2 + h_3}{2} + h_{23} + a_{2,u} = 97.71 \text{ mm}$$

$$EI_{ef,u} = E_1 I_1 + E_2 I_2 + E_3 I_3 + \gamma_{1,u} E_1 A_1 a_{1,u}{}^2 + \gamma_2 E_2 A_2 a_{2,u}{}^2 + \gamma_3 E_3 A_3 a_{3,u}{}^2 = 6.99 \text{ MN·m}^2$$

where A_i and I_i are the area and the second moment of area of the i^{th} element in Fig. 6, respectively, and $\gamma_2 = 1$.

Verifications:

Stresses in the glulam member (element 1)

$$\sigma_{m,1,u} = \frac{0.5 \cdot E_1 h_1 M_{ULS,d}}{EI_{ef,u}} = 4.65 \text{ MPa} \qquad \text{(bending stress)}$$

$$\sigma_{1,u} = \frac{\gamma_{1,u} E_1 a_{1,u} M_{ULS,d}}{EI_{ef,u}} = 1.49 \text{ MPa} \qquad \text{(axial compressive stress)}$$

Compressive stress at the top of the glulam beam: $\sigma_{m,1,u} + \sigma_{1,u} = 4.65 + 1.49 = 6.14$ MPa

$$\frac{\sigma_{m,1,u} + \sigma_{1,u}}{f_{m,1,d}} = \frac{6.14}{22.75} = 0.27 < 1 \quad \rightarrow \qquad \text{satisfactory}$$

Tensile stress at the bottom of the glulam beam: $\sigma_{m,1,u} - \sigma_{1,u} = 4.65 - 1.49 = 3.16$ MPa

$$\frac{\sigma_{m,1,u} - \sigma_{1,u}}{f_{m,1,d}} = \frac{3.16}{22.75} = 0.14 < 1 \quad \rightarrow \qquad \text{satisfactory}$$

Maximum shear stress in the glulam beam $\tau_{1,\max}$, assuming that the glulam beam takes all the shear stresses:

$$\tau_{1,\max} = 1.5(V_{ULS,d} / A_1) = 0.50 \text{ MPa}$$

$$\frac{\tau_{1,\max}}{f_{v,1,d}} = \frac{0.50}{2.53} = 0.20 < 1 \qquad \rightarrow \qquad \text{satisfactory}$$

Stresses in the CLT panel (element 3)

$$\sigma_{m,3,u} = \frac{0.5 \cdot E_3 h_3 M_{ULS,d}}{EI_{ef,u}} = 0.24 \text{ MPa} \qquad \text{(bending stress)}$$

$$\sigma_{3,u} = \frac{\gamma_3 E_3 a_{3,u} M_{ULS,d}}{EI_{ef,u}} = 2.27 \text{ MPa} \qquad \text{(axial tensile stress)}$$

Tensile stress at the bottom of the CLT panel: $\sigma_{3,u} + \sigma_{m,3,u} = 2.27 + 0.24 = 2.51$ MPa

The axial tensile stress being dominant compared to the bending stress in this case, it is suggested to conservatively carry out the verification with respect to the design tensile strength $f_{t,0,3,d}$.

$$\frac{\sigma_{3,u} + \sigma_{m,3,u}}{f_{t,0,3,d}} = \frac{2.51}{8.96} = 0.28 < 1 \qquad \rightarrow \qquad \text{satisfactory}$$

Rolling shear stress in the cross layer (between element 2 and element 3):

The rolling shear stress is assumed uniform over the depth of the cross layer and is assumed equal to the shear stress at the interface with the layers above and underneath. The rolling shear stress in the cross layer is expressed with this assumption as:

$$\tau_{v,23} = \frac{\gamma_3 \cdot E_3 \cdot A_3 \cdot a_{3.u}}{EI_{ef,u} \cdot b_3} V_{ULS,d} = 28.35 \text{ kPa}$$

$$\frac{\tau_{v,23}}{f_{R,d}} = \frac{28.35 \cdot 10^{-3}}{0.80} = 0.04 < 1 \quad \rightarrow \quad \text{satisfactory}$$

Considering the more conservative assumption of shear stresses distributed down to the cross layer from the glulam beam area with a 45 degree angle, therefore virtually reducing the effective width of the cross layer. The rolling shear stress is calculated,

$$\tau_{v,23,alt} = \frac{\gamma_3 \cdot E_3 \cdot A_3 \cdot a_{3.u}}{EI_{ef,u} \cdot (b_1 + 2 \cdot h_2)} V_{ULS,d} = 126.5 \text{ kPa}$$

$$\frac{\tau_{v,23,alt}}{f_{R,d}} = \frac{126.5 \cdot 10^{-3}}{0.80} = 0.16 < 1 \quad \rightarrow \quad \text{satisfactory}$$

Maximum force in a single shear connection:

$$F_{sc,u} = \frac{\gamma_{1,u} E_1 A_{1,u} s}{EI_{ef,u}} V_{ULS,d} = 11.86 \text{ kN}$$

$$\frac{F_{sc,u}}{F_{Rd}} = \frac{11.86}{18.93} = 0.63 < 1 \quad \rightarrow \quad \text{satisfactory}$$

A.2.2 ULS long-term:

The creep factors to consider for the long-term verification of the composite beam being different depending on the duration of the load, the load combination for the ULS long-term verification is separated in two parts, the quasi-permanent part which is acting during the entire service life $w_{SLS,p}$, and the instantaneous part of the ULS load case $w_{ULS,fin}$ which is only acting at the end life of the structure for the verification of the strength in the long-term conditions and which corresponds to $w_{ULS} - w_{SLS,p}$. The effects of these separated load cases are then superimposed to carry out the necessary verifications.

Quasi permanent combination: $G_k + \psi_2 \cdot Q_k$

Load case: $w_{SLS,p} = \left(G_k + \psi_2 \cdot Q_k\right) \cdot b_{unit} = \left(1.80 + 0.3 \cdot 2.00\right) \cdot 0.58 = 1.39$ kN/m

Design bending moment: $M_{SLS,p} = \dfrac{w_{SLS,p} \cdot L^2}{8} = 7.13$ kN·m (maximum design bending moment)

Design shear force: $V_{SLS,p} = \dfrac{w_{SLS,p} \cdot L}{2} = 4.45$ kN (maximum design shear force)

Bending stiffness of the composite beam:

$$\gamma_{1,s,p} = \left(1 + \pi^2 \frac{E_{1,fin} A_1}{K_{1,s,fin} L^2}\right)^{-1} = 0.481$$

$$\gamma_{3,s,p} = \left(1 + \pi^2 \frac{E_{3,fin} A_3 h_{23}}{G_{R,fin} b_3 L^2}\right)^{-1} = \gamma_3 = 0.979$$

$$a_{2,s,p} = \frac{\gamma_{1,s,p} E_{1,fin} A_1 \left(\frac{h_1 + h_2}{2}\right) - \gamma_3 E_{3,fin} A_3 \left(\frac{h_2 + h_3}{2} + h_{23}\right)}{\gamma_{1,s,p} E_{1,fin} A_1 + \gamma_2 E_{2,fin} A_2 + \gamma_3 E_{3,fin} A_3} = 59.82 \text{ mm}$$

$$a_{1,s,p} = \frac{h_1 + h_2}{2} - a_{2,s,p} = 107.68 \text{ mm}$$

$$a_{3,s,p} = \frac{h_2 + h_3}{2} + h_{23} + a_{2,s,p} = 99.82 \text{ mm}$$

$$EI_{ef,s,p} = E_{1,fin} I_1 + E_{2,fin} I_2 + E_{3,fin} I_3 + \gamma_{1,s,p} E_{1,fin} A_1 a_{1,s,p}{}^2 + \gamma_2 E_{2,fin} A_2 a_{2,s,p}{}^2 + \gamma_3 E_{3,fin} A_3 a_{3,s,p}{}^2 = 4.43 \text{ MN·m}^2$$

Instantaneous part of the long-term ULS load case: $w_{ULS,fin,inst} = w_{ULS} - w_{SLS,p}$

$w_{ULS,fin,inst} = w_{ULS} - w_{SLS,p} = 2.94 - 1.39 = 1.55$ kN/m

Design bending moment: $M_{ULS,fin,inst} = w_{ULS,fin,inst} \cdot L^2 / 8 = 7.93$ kN·m

Design shear force: $V_{ULS,fin,inst} = w_{ULS,fin,inst} \cdot L / 2 = 4.96$ kN

Bending stiffness of the composite beam:

$$\gamma_{1,u,fin} = \left(1 + \pi^2 \frac{E_{1,fin} A_1}{K_{1,u,fin} L^2}\right)^{-1} = 0.382$$

$$\gamma_{3,u,fin} = \left(1 + \pi^2 \frac{E_{3,fin} A_3 h_{23}}{G_{R,fin} b_3 L^2}\right)^{-1} = \gamma_{3,s,fin} = \gamma_3 = 0.979$$

$$a_{2,u,fin} = \frac{\gamma_{1,u,fin} E_{1,fin} A_1 \left(\frac{h_1 + h_2}{2}\right) - \gamma_3 E_{3,fin} A_3 \left(\frac{h_2 + h_3}{2} + h_{23}\right)}{\gamma_{1,u,fin} E_{1,fin} A_1 + \gamma_2 E_{2,fin} A_2 + \gamma_3 E_{3,fin} A_3} = 49.48 \text{ mm}$$

$$a_{1,u,fin} = \frac{h_1 + h_2}{2} - a_{2,u,fin} = 118.02 \text{ mm}$$

$$a_{3,u,fin} = \frac{h_2 + h_3}{2} + h_{23} + a_{2,u,fin} = 89.48 \text{ mm}$$

$$EI_{ef,u,fin} = E_{1,fin} I_1 + E_{2,fin} I_2 + E_{3,fin} I_3 + \gamma_{1,u,fin} E_{1,fin} A_1 a_{1,u,fin}^2 + \gamma_2 E_{2,fin} A_2 a_{2,u,fin}^2 + \gamma_3 E_{3,u,fin} A_3 a_{3,u,fin}^2 = 4.12 \text{ MN·m}^2$$

Verifications:

The design strength of the different timber members used is the same as for the short-term verifications according to the clause 3.1.3 (2) in the EC5 [9]. Long-term design strength values would have been necessary for a load combination consisting of permanent load only.

Stresses in the glulam member (element 1):

Due to the quasi permanent part of the load combination:

$$\sigma_{m,1,s,p} = \frac{0.5 \cdot E_{1,fin} h_1 M_{SLS,p}}{EI_{ef,s,p}} = 2.17 \text{ MPa} \qquad \text{(bending stresses)}$$

$$\sigma_{1,s,p} = \frac{\gamma_{1,s,p} E_{1,fin} a_{1,s,p} M_{SLS,p}}{EI_{ef,s,p}} = 0.71 \text{ MPa} \qquad \text{(axial compressive stresses)}$$

Due to the instantaneous part of the ULS load combination at the end life:

$$\sigma_{m,1,u,fin,inst} = \frac{0.5 \cdot E_{1,fin} h_1 M_{ULS,fin,inst}}{EI_{ef,u,fin}} = 2.59 \text{ MPa} \qquad \text{(bending stresses)}$$

$$\sigma_{1,u,fin,inst} = \frac{\gamma_{1,u,fin} E_{1,fin} a_{1,u,fin} M_{ULS,fin,inst}}{EI_{ef,u,fin}} = 0.74 \text{ MPa} \qquad \text{(axial compressive stresses)}$$

Superimposition of the compressive stresses at the top of the glulam beam:

$$\sigma_{m,1,s,p} + \sigma_{m,1,u,fin,inst} + \sigma_{1,s,p} + \sigma_{1,u,fin,inst} = 2.17 + 2.59 + 0.71 + 0.74 = 6.22 \text{ MPa}$$

$$\frac{\sigma_{m,1,s,p} + \sigma_{m,1,u,fin,inst} + \sigma_{1,s,p} + \sigma_{1,u,fin,inst}}{f_{m,1,d}} = \frac{6.22}{22.75} = 0.27 < 1 \rightarrow \qquad \text{satisfactory}$$

Superimposition of the tensile stresses at the bottom of the glulam beam:

$$\sigma_{m,1,s,p} + \sigma_{m,1,u,fin,inst} - \sigma_{1,s,p} - \sigma_{1,u,fin,inst} = 2.17 + 2.59 - 0.71 - 0.74 = 3.31 \text{ MPa}$$

$$\frac{\sigma_{m,1,s,p} + \sigma_{m,1,u,fin,inst} - \sigma_{1,s,p} - \sigma_{1,u,fin,inst}}{f_{m,1,d}} = \frac{3.31}{22.75} = 0.15 < 1 \rightarrow \quad \text{satisfactory}$$

Maximum shear stresses in the glulam beam $\tau_{1,\max,fin}$, assuming that the glulam beam takes all the shear stresses remains the same as for the short term ULS load case:

$$\tau_{1,\max,fin} = 1.5(V_{ULS,d} / A_1) = 0.50 \text{ MPa}$$

$$\frac{\tau_{1,\max,fin}}{f_{v,1,d}} = \frac{0.50}{2.53} = 0.20 < 1 \quad \rightarrow \quad \text{satisfactory}$$

Stresses in the CLT panel (element 3):

Due to the quasi permanent part of the load combination

$$\sigma_{m,3,s,p} = \frac{0.5 \cdot E_{3,fin} h_3 M_{SLS,p}}{EI_{ef,s,p}} = 0.11 \text{ MPa} \quad \text{(bending stresses)}$$

$$\sigma_{3,s,p} = \frac{\gamma_3 E_{3,fin} a_{3,s,p} M_{SLS,p}}{EI_{ef,s,p}} = 1.08 \text{ MPa} \quad \text{(axial compressive stresses)}$$

Due to the instantaneous part of the ULS load combination at the end life

$$\sigma_{m,3,u,fin,inst} = \frac{0.5 \cdot E_{3,fin} h_3 M_{ULS,fin,inst}}{EI_{ef,u,fin}} = 0.13 \text{ MPa} \quad \text{(bending stresses)}$$

$$\sigma_{3,u,fin,inst} = \frac{\gamma_3 E_{3,fin} a_{3,u,fin} M_{ULS,fin,inst}}{EI_{ef,u,fin}} = 1.16 \text{ MPa} \quad \text{(axial compressive stresses)}$$

Superimposition of the tensile stresses at the bottom of the glulam beam (verification with respect to the tensile strength):

$$\sigma_{m,3,s,p} + \sigma_{m,3,u,fin,inst} + \sigma_{3,s,p} + \sigma_{3,u,fin,inst} = 0.11 + 0.13 + 1.08 + 1.16 = 2.48 \text{ MPa}$$

$$\frac{\sigma_{m,3,s,p} + \sigma_{m,3,u,fin,inst} + \sigma_{3,s,p} + \sigma_{3,u,fin,inst}}{f_{t,0,3,d}} = \frac{2.48}{8.96} = 0.28 < 1 \rightarrow \quad \text{satisfactory}$$

Rolling shear stress in the CLT cross layer:

$$\tau_{v,23,fin} = \frac{\gamma_3 \cdot E_{3.fin} \cdot A_3 \cdot a_{3.s.fin}}{EI_{ef,s,p} \cdot b_3} V_{SLS,p} + \frac{\gamma_3 \cdot E_{3.fin} \cdot A_3 \cdot a_{3.u.fin}}{EI_{ef,u,fin} \cdot b_3} V_{ULS,fin,inst} = 28.00 \text{ kPa}$$

$$\frac{\tau_{v,23,fin}}{f_{R,d}} = \frac{28.0 \cdot 10^{-3}}{0.80} = 0.03 < 1 \quad \rightarrow \quad \text{satisfactory}$$

Considering the more conservative assumption of shear stresses distributed down to the cross layer from the glulam beam area with a 45 degree angle, therefore virtually reducing the effective width of the cross layer. The rolling shear stress is calculated,

$$\tau_{v,23,fin,alt} = \frac{\gamma_3 \cdot E_{3.fin} \cdot A_3 \cdot a_{3.s.fin}}{EI_{ef,s,fin} \cdot (b_1 + 2 \cdot h_2)} V_{SLS,p} + \frac{\gamma_3 \cdot E_{3.fin} \cdot A_3 \cdot a_{3.u.fin}}{EI_{ef,u,fin} \cdot (b_1 + 2 \cdot h_2)} V_{ULS,fin,inst} = 124.9 \text{ kPa}$$

$$\frac{\tau_{v,23,fin,alt}}{f_{R,d}} = \frac{124.9 \cdot 10^{-3}}{0.80} = 0.16 < 1 \quad \rightarrow \quad \text{satisfactory}$$

Maximum force in the shear connection:

$$F_{sc,uls,fin} = \frac{\gamma_{1,s,p} E_{1,fin} A_1 a_{1,s,fin} s}{EI_{ef,s,fin}} V_{SLS,p} + \frac{\gamma_{1,u,fin} E_{1,fin} A_1 a_{1,u,fin} s}{EI_{ef,u,fin}} V_{ULS,fin,inst} = 11.60 \text{ kN}$$

$$\frac{F_{sc,uls,fin}}{F_{Rd}} = \frac{11.60}{18.93} = 0.61 < 1 \quad \rightarrow \quad \text{satisfactory}$$

A.2.3. SLS short term:

Characteristic combination: $G_k + Q_k$

The load case for the single beam unit is given by w_{SLS} :

$$w_{SLS} = (G_k + Q_k) \cdot b_{unit} = (1.80 + 2.00) \cdot 0.58 = 2.2 \text{ kN/m}$$

Design bending moment: $M_{SLS,d} = (w_{SLS} \cdot L^2)/8 = 11.28 \text{ kN·m}$

Design shear force: $V_{SLS,d} = (w_{SLS} \cdot L)/2 = 7.05 \text{ kN}$

Bending stiffness of the composite beam:

$$\gamma_{1,s} = \left(1 + \pi^2 \frac{E_1 A_1}{K_{1,s} L^2}\right)^{-1} = 0.56$$

$$a_{2,s} = \frac{\gamma_{1,s} E_1 A_1 \left(\frac{h_1 + h_2}{2}\right) - \gamma_3 E_3 A_3 \left(\frac{h_2 + h_3}{2} + h_{23}\right)}{\gamma_{1,s} E_1 A_1 + \gamma_2 E_2 A_2 + \gamma_3 E_3 A_3} = 66.87 \text{ mm}$$

$$a_{1,s} = \frac{h_1 + h_2}{2} - a_{2,s} = 100.63 \text{ mm}$$

$$a_{3,s} = \frac{h_2 + h_3}{2} + h_{23} + a_{2,s} = 106.87 \text{ mm}$$

$$EI_{ef,s} = E_1 I_1 + E_2 I_2 + E_3 I_3 + \gamma_{1,s} E_1 A_1 a_{1,s}^2 + \gamma_2 E_2 A_2 a_{2,s}^2 + \gamma_3 E_3 A_3 a_{3,s}^2 = 7.42 \text{ MN·m}^2$$

Verifications:

Instantaneous deflection:

$$u_{inst,s} = \frac{5 \cdot w_{SLS} L^4}{384 \cdot EI_{ef,s}} = 6.49 \text{ mm} < u_{inst,\lim} = \frac{L}{400} = 16 \text{ mm.}$$

$$\frac{u_{inst,s}}{u_{inst,\lim}} = 0.44 < 1 \quad \rightarrow \quad \text{satisfactory}$$

Maximum force in the shear connection:

$$F_{sc,sls} = \frac{\gamma_{1,s} E_1 A_1 a_{1,s} s}{EI_{ef,s}} V_{SLS} = 9.36 \text{ kN}$$

$$\frac{F_{sc,sls}}{F_{Rd}} = \frac{9.36}{18.93} = 0.49 < 1 \quad \rightarrow \quad \text{satisfactory}$$

Vibration:

For the estimation of the fundamental frequency f_1 of residential floors according to the EC5 and Finnish National Annex (NA), the mass *m* of the floor per square meter should be considered equal to the self-weight of the floor element (structural part and finishes) to which a mass of 30 kg/m^2 is added to account for the permanent part of the service load [14], therefore:

$m = \frac{G_k}{g} + 30 kg/m^2 = 213.55$ kg/m^2 with *g* the gravitational constant, giving the fundamental frequency for a simply supported floor:

$$f_1 = \frac{\pi}{2 \cdot L^2} \sqrt{\frac{\left(EI_{ef,s}\right)_l}{m}} = 9.39 \text{ Hz} \geq f_{1,\lim} = 9 \text{ Hz} \quad \rightarrow \quad \text{satisfactory}$$

where $\left(EI_{ef,s}\right)_l = \frac{EI_{ef,s}}{b_{unit}}$ is the equivalent plate bending stiffness of the floor about an axis perpendicular to the beam direction [Nm^2/m].

For residential floors having a fundamental frequency higher the 9 Hz, and according to the EC5 and Finnish NA, the unit velocity response "*v*" and the deflection "δ_{1kN}" under a static point load of 1 kN should satisfy certain requirements.

The unit impulse velocity response *v* is calculated:

$$v = \frac{4(0.4 + 0.6 n_{40})}{m \cdot B \cdot L + 200} = 3.64 \times 10^{-3} \text{ m/(N·s}^2\text{)}$$

where

$$n_{40} = \left\{ \left(\left(\frac{40}{f_1} \right)^2 - 1 \right) \left(\frac{B}{L} \right)^4 \frac{\left(EI_{ef,s} \right)_l}{\left(EI \right)_b} \right\}^{0.25} = 5.96$$

$\left(EI \right)_b = \frac{h_{23}^{\ 3}}{12} E_3$ is the equivalent plate bending stiffness of the floor about an axis parallel to the beam span [Nm^2/m], taken conservatively as the bending stiffness of the transverse CLT layer (height h_{23}) about the axis parallel to the beam span.

B = 2.9 m the floor element width considered (a CLT panel with 5 glulam beams and spacing of 580 mm)

The expression $\nu \le b^{(f_1 \zeta - 1)}$ should be verified, with, b = 150 according to the Finnish NA.

Assuming a conservative modal damping ratio ζ = 1% (higher values, 2% or 3 %, could be considered for this type of floor element):

$$\frac{\nu}{b^{(f_1 \zeta - 1)}} = 0.34 < 1 \quad \rightarrow \quad \text{satisfactory}$$

The maximum deflection caused by a static concentrated loading P = 1 kN should not exceed 0.5 mm according to the Finnish NA and is calculated:

$$\delta_{1\text{kN}} = \min \left\{ \frac{PL^2}{42 k_\delta \left(EI_{ef,s} \right)_l} \; ; \; \frac{PL^3}{42 EI_{ef,s}} \right\} = 0.49 \text{ mm} < 0.5 \text{ mm} \quad \rightarrow \quad \text{satisfactory}$$

where

$$k_\delta = \min \left\{ \frac{B}{L} \; ; \; \sqrt[4]{\frac{\left(EI_{ef,s} \right)_l}{\left(EI \right)_b}} \right\} = 0.17$$

It can be noted that the deflection criteria under the 1 kN concentrated load is just fulfilled considering the most conservative assumption which assumes that the bending stiffness $(EI)_b$ about an axis perpendicular to the span is obtained from the transverse CLT layer only. The contribution of the additional floor finishes layers (i.e. floating floor made of a cement screed over a wood based skin plate) could be considered in addition and would allow to distribute even more the concentrated load over the floor width. This may easily lead to a k_δ value twice as high, reducing the deflection $\delta_{1\text{kN}}$ in the same proportions.

A.2.4. SLS long-term

For the long term SLS verification the deflections $u_{\text{fin,p}}$ under the quasi-permanent load combination $w_{\text{SLS,p}}$, and $u_{\text{fin,r}}$ under the characteristic combination w_{SLS} (rare combination) are calculated using the bending stiffness for the long-term serviceability $EI_{ef,s,p}$.

$$u_{fin,p} = \frac{5 \cdot w_{SLS,p} L^4}{384 \cdot EI_{ef,s,p}} = 6.87 \text{ mm} < u_{net,fin,\text{lim}} = \frac{L}{300} = 21.33 \text{ mm}$$

$$u_{fin,r} = \frac{5 \cdot w_{SLS,r} L^4}{384 \cdot EI_{ef,s,p}} = 10.87 \text{ mm} < u_{net,fin,\lim} = \frac{L}{300} = 21.33 \text{ mm}$$

$$\frac{u_{fin,p}}{u_{net,fin,\lim}} = 32.2\ \% \text{ and } \frac{u_{fin,r}}{u_{net,fin,\lim}} = 51.0\ \% \quad \rightarrow \quad \text{satisfactory}$$

Maximum force in the shear connection:

Quasi permanent combination:

$$F_{sc,sls} = \frac{\gamma_{1,s,p} E_{1,fin} A_1 a_{1,s,fin} s}{EI_{ef,s,fin}} V_{SLS,p} = 9.1 \text{ kN}$$

$$\frac{F_{sc,sls}}{F_{Rd}} = \frac{9.1}{18.93} = 0.48 < 1 \quad \rightarrow \quad \text{satisfactory}$$

Rare combination:

$$F_{sc,sls} = \frac{\gamma_{1,s,p} E_{1,fin} A_1 a_{1,s,fin} s}{EI_{ef,s,fin}} V_{SLS} = 14.41 \text{ kN}$$

$$\frac{F_{sc,sls}}{F_{Rd}} = \frac{14.41}{18.93} = 0.76 < 1 \quad \rightarrow \quad \text{satisfactory}$$

Design summary:

		ULS short term	ULS long term		
		Fundamental combination w_{ULS}	Quasi-perm. part $w_{SLS,p}$	Instantaneous part $w_{ULS,fin,inst}$	Total (w_{ULS}) $w_{SLS,p} + w_{ULS,fin,inst}$
Load case (kN/m)	w	2.94	1.39	1.55	2.94
Design moment (kN·m)	M_d	15.06	7.13	7.93	15.06
Design shear force (kN)	V_d	9.41	4.45	4.96	9.41
Bending stiffness (MN·m^2)	EI_{ef}	6.99	4.43	4.12	-
Element 1 (Glulam beam)					
Bending stress (MPa)	$\sigma_{m,1}$	4.65	2.17	2.59	4.76
Axial compressive stress (MPa)	σ_1	1.49	0.71	0.74	1.45
Compressive stress check at the top	$\frac{\sigma_{m,1}+\sigma_1}{f_{m,1,d}}$	$\frac{6.14}{22.75}=0.27<1$	2.88	3.34	$\frac{6.22}{22.75}=0.27<1$
Tensile stress check at the bottom	$\frac{\sigma_{m,1}-\sigma_1}{f_{m,1,d}}$	$\frac{3.16}{22.75}=0.14<1$	1.46	1.85	$\frac{3.31}{22.75}=0.15<1$
Shear stress check at $h_1/2$ (MPa)	$\frac{\tau_{1,max}}{f_{v,1,d}}$	$\frac{0.50}{2.53}=0.20<1$	-	-	$\frac{0.50}{2.53}=0.20<1$
Element 3 (CLT bottom layer)					
Bending stress (MPa)	$\sigma_{m,3}$	0.24	0.11	0.13	0.24
Axial compressive stress (MPa)	σ_3	2.27	1.08	1.16	2.24
Tensile stress check at the bottom	$\frac{\sigma_3+\sigma_{m,3}}{f_{m,3,d}}$	$\frac{2.51}{8.96}=0.28<1$	1.19	-	$\frac{2.48}{8.96}=0.28<1$
Rolling shear stress in the cross layer (kPa)	$\tau_{v,23}$	28.35	13.52	14.48	28.00

Verification (MPa)	$\frac{\tau_{v,23}}{f_{R,d}}$	$\frac{28.35 \cdot 10^{-3}}{0.80} = 0.04 < 1$	-	-	$\frac{28.00 \cdot 10^{-3}}{0.80} = 0.03 < 1$
Rolling shear stress in the cross layer (MPa)	$\tau_{v,23,alt}$	0.126	0.060	0.065	0.12
Verification (MPa)	$\frac{\tau_{v,23,alt}}{f_{R,d}}$	$\frac{0.126}{0.80} = 0.16 < 1$	-	-	$\frac{0.12}{0.80} = 0.16 < 1$
Maximum force in a single connector (kN)	$F_{sc,uls}$	11.86	5.69	5.91	11.60
Shear connector resistance check	$\frac{F_{sc,uls}}{F_{Rd}}$	$\frac{11.86}{18.93} = 0.63 < 1$	-	-	$\frac{11.60}{18.93} = 0.61 < 1$

		SLS short term	**SLS long term**	
		Characteristic combination	Quasi-perm. combination	Rare combination
		w_{SLS}	$w_{SLS,p}$	w_{SLS}
Load case (kN/m)	w	2.2	1.39	2.2
Design moment (kN·m)	M_d	11.28	7.13	11.28
Design shear force (kN)	V_d	7.05	4.45	7.05
Bending stiffness (MN·m^2)	EI_{ef}	7.42	4.43	4.43
Mid-span deflection (mm)	u_{inst}	6.49	6.87	10.87
Deflection limit (mm)	$u_{\lim}$	$\frac{L}{400} = 16$	$\frac{L}{300} = 21.3$	$\frac{L}{300} = 21.3$
Instantaneous deflection check	$\frac{u_{inst}}{u_{\lim}}$	0.44 < 1	0.32 < 1	0.51 < 1
Fundamental frequency (Hz)	f_1	9.39 > 9	-	-
Impulse velocity response check	$\frac{v}{b^{(f_1\zeta-1)}}$	0.36 < 1	-	-
Deflection under 1 kN concentrated force (mm)	δ_{1kN}	0.49 < 0.5	-	-
Maximum force in a single connector (kN)	$F_{sc,sls}$	9.36	9.10	14.41
	$\frac{F_{sc,sls}}{F_{Rd}}$	0.49 < 1	0.48 < 1	0.76 < 1

Appendix B: Additional load-deflection and slip measurements

For each test specimen of each test series, four diagrams are presented. On left, the entire load-deflection curve at mid-span with an enlarged view of the same curve at the bottom.
On the top right, the slip measurements recorded at each position (p#) along the composite beam length (Fig. 13), and at the bottom, an enlarged view of the same curve.

Series B1_S (Inclined screws only)

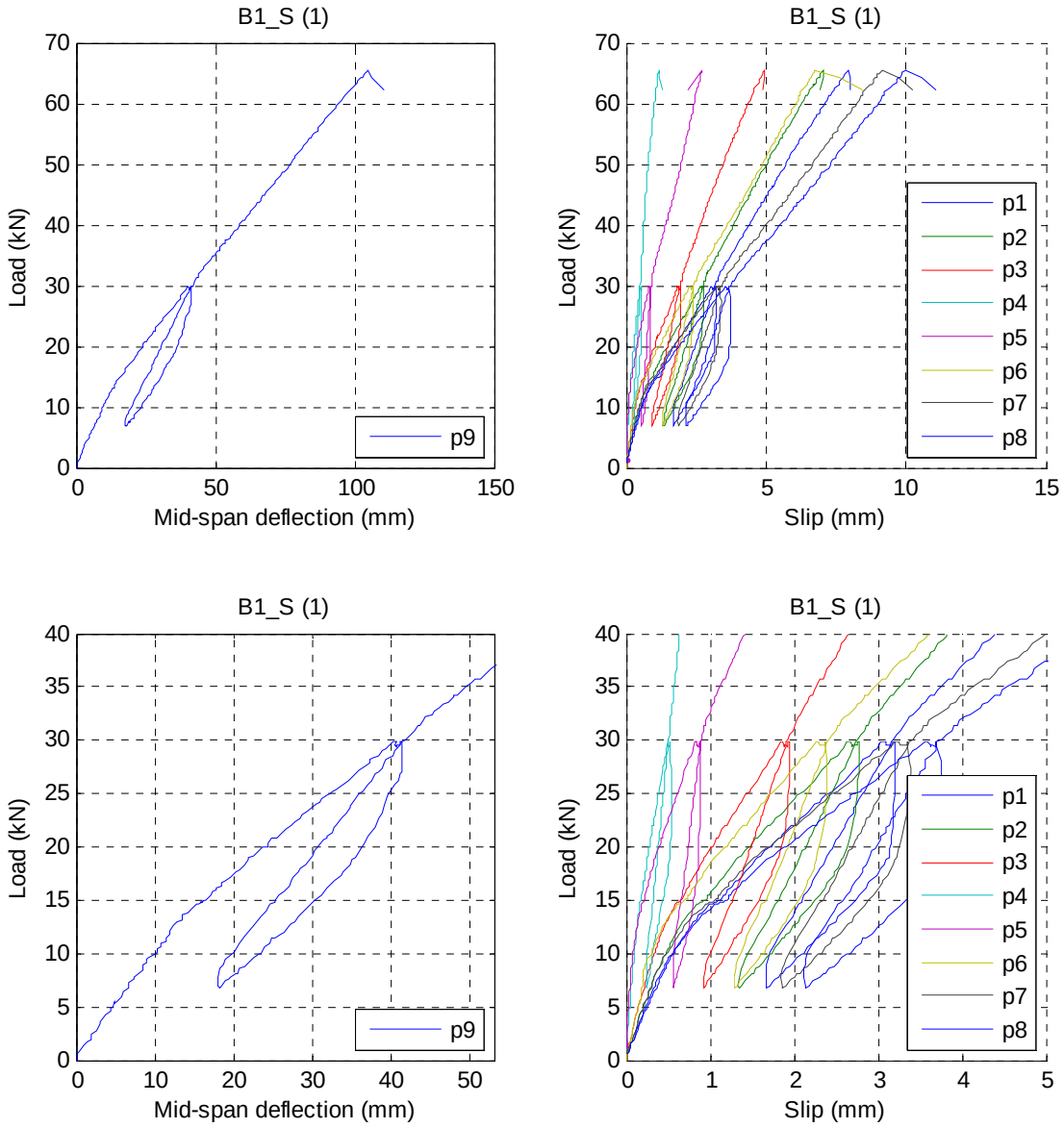

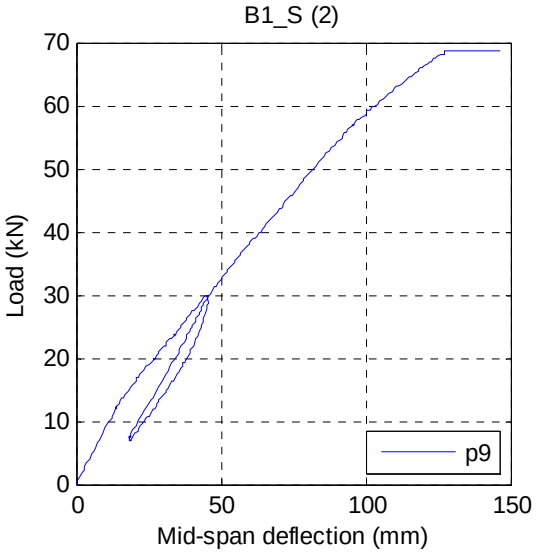
B1_S (2)
Load (kN)
Mid-span deflection (mm)
p9

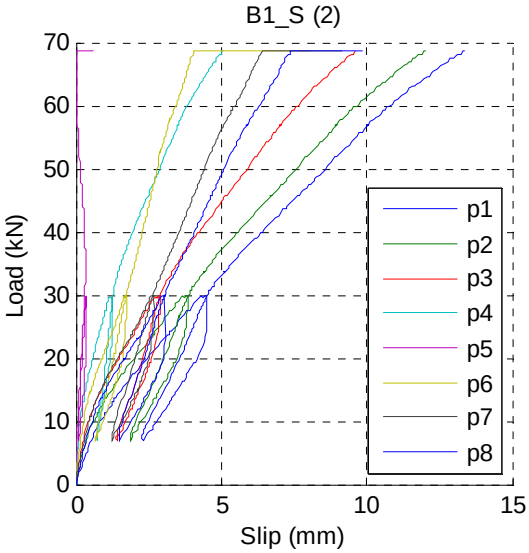
B1_S (2)
Load (kN)
Slip (mm)
p1
p2
p3
p4
p5
p6
p7
p8

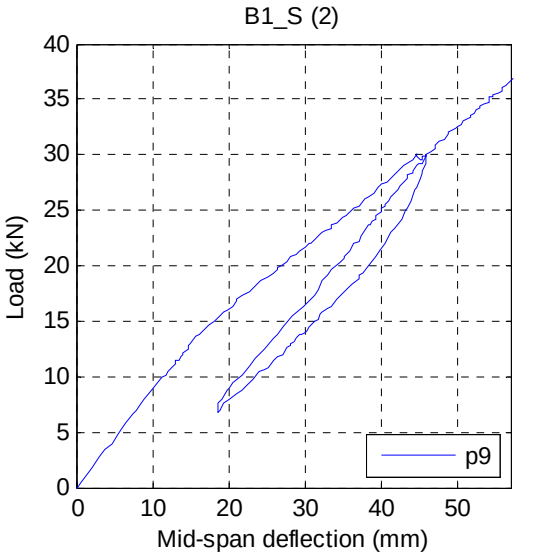
B1_S (2)
Load (kN)
Mid-span deflection (mm)
p9

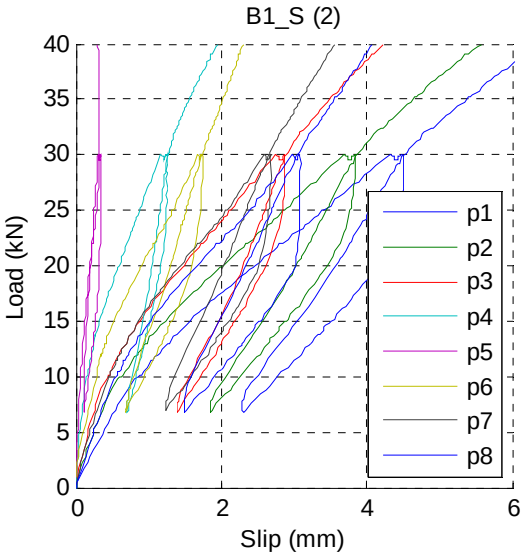
B1_S (2)
Load (kN)
Slip (mm)
p1
p2
p3
p4
p5
p6
p7
p8

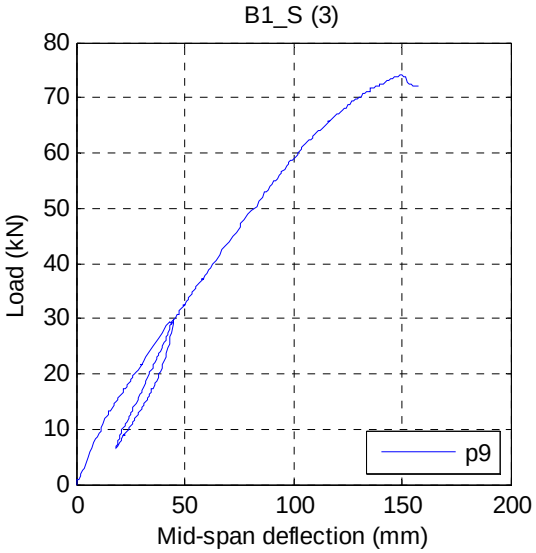
B1_S (3)
Load (kN)
Mid-span deflection (mm)
p9

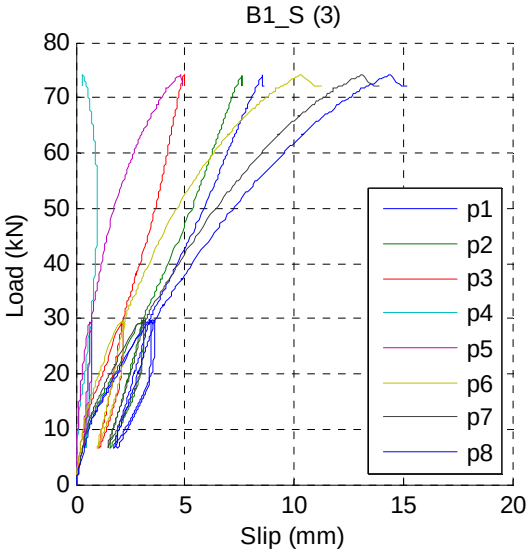
B1_S (3)
Load (kN)
Slip (mm)
p1
p2
p3
p4
p5
p6
p7
p8

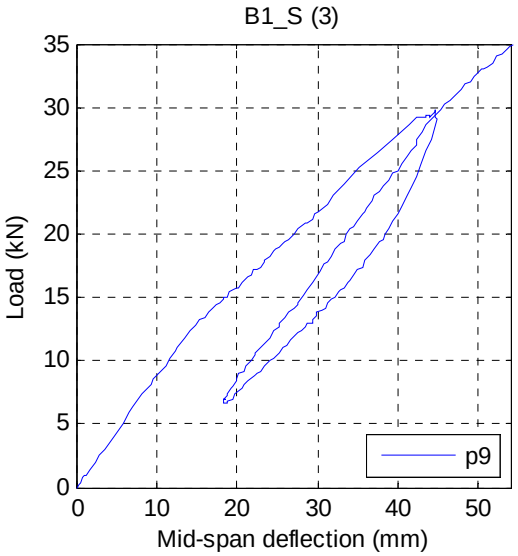
B1_S (3)
Load (kN)
Mid-span deflection (mm)
p9

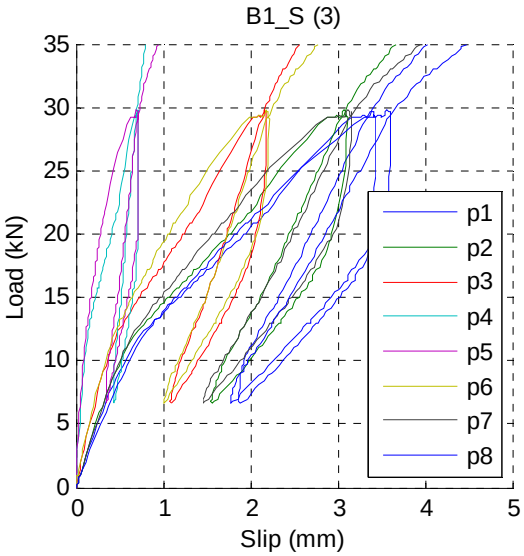
B1_S (3)
Load (kN)
Slip (mm)
p1
p2
p3
p4
p5
p6
p7
p8

Series B2_NP (Double-sided nail plates only)

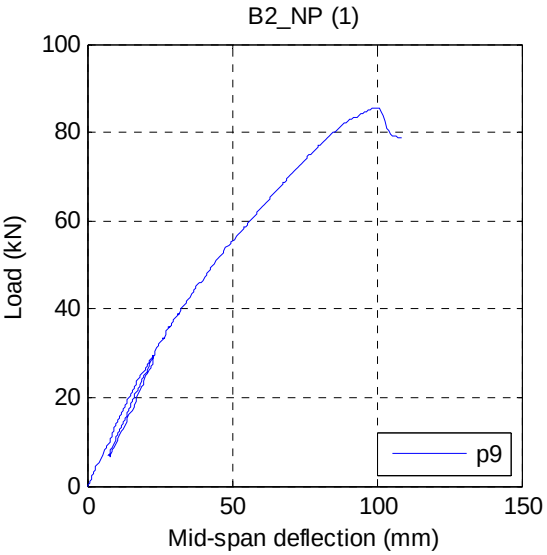

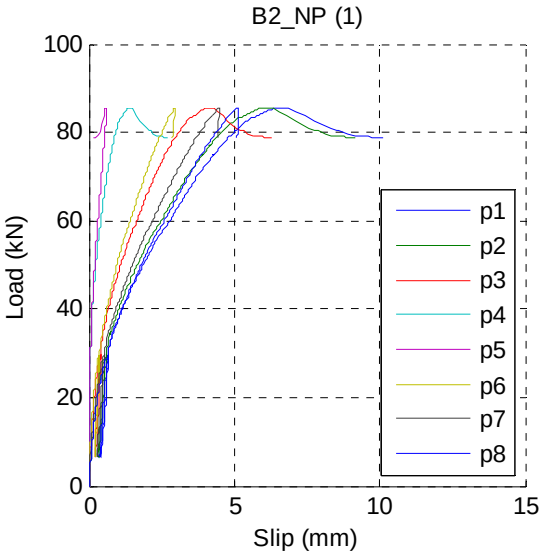

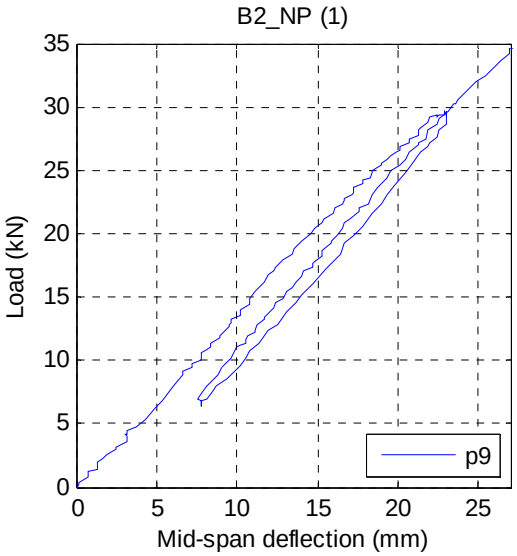

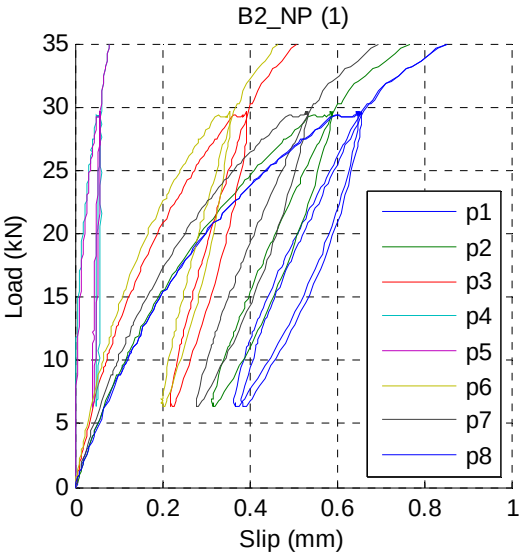

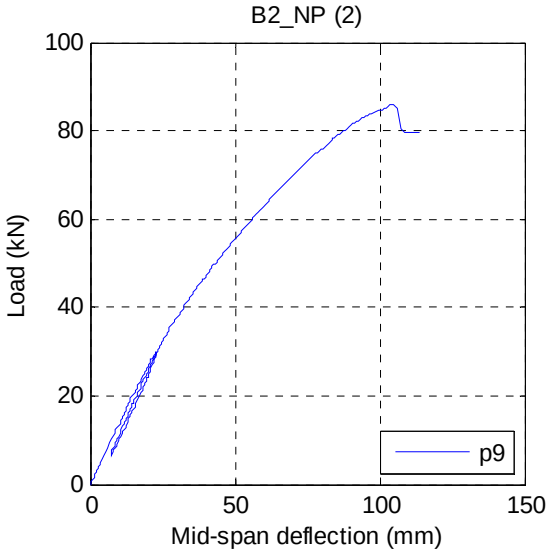
B2_NP (2)
Load (kN)
Mid-span deflection (mm)
p9

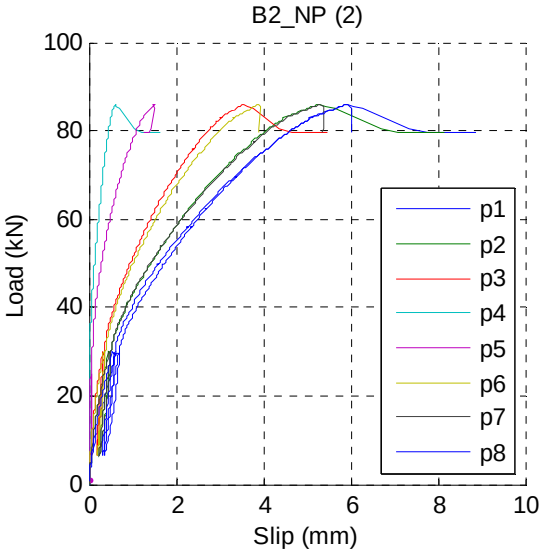
B2_NP (2)
Load (kN)
Slip (mm)
p1
p2
p3
p4
p5
p6
p7
p8

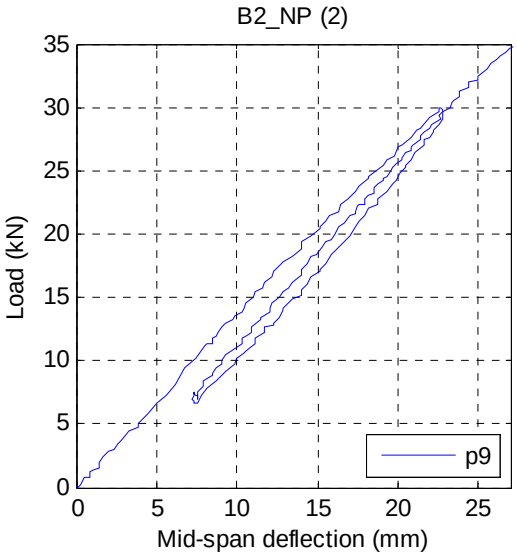
B2_NP (2)
Load (kN)
Mid-span deflection (mm)
p9

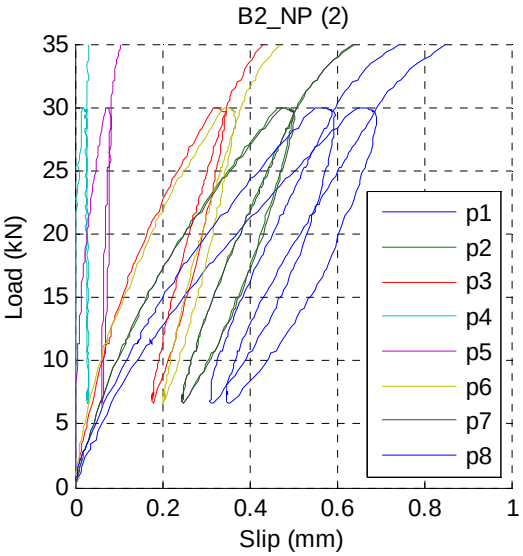
B2_NP (2)
Load (kN)
Slip (mm)
p1
p2
p3
p4
p5
p6
p7
p8

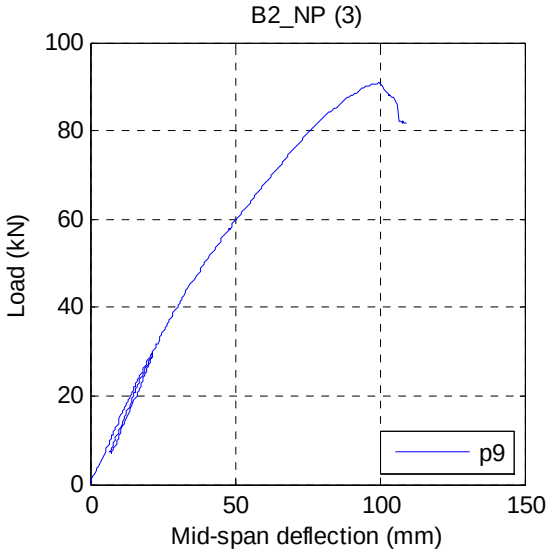
B2_NP (3)
Load (kN)
Mid-span deflection (mm)
p9

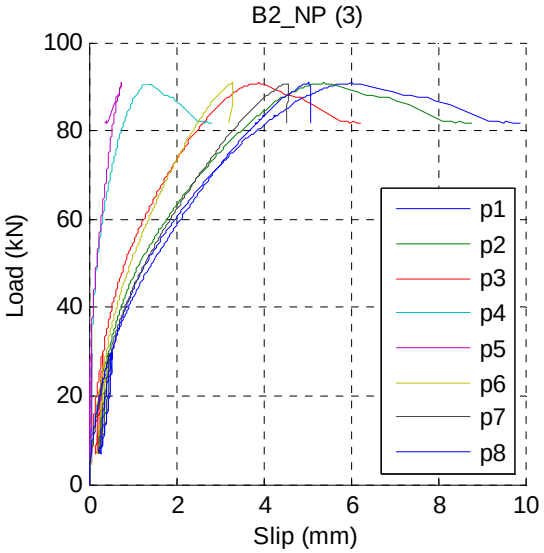
B2_NP (3)
Load (kN)
Slip (mm)
p1
p2
p3
p4
p5
p6
p7
p8

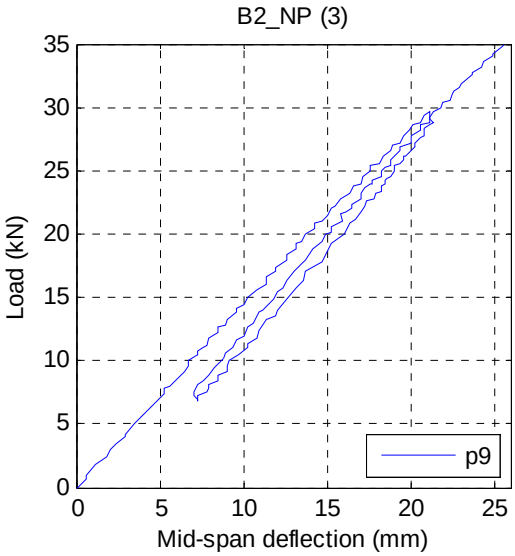
B2_NP (3)
Load (kN)
Mid-span deflection (mm)
p9

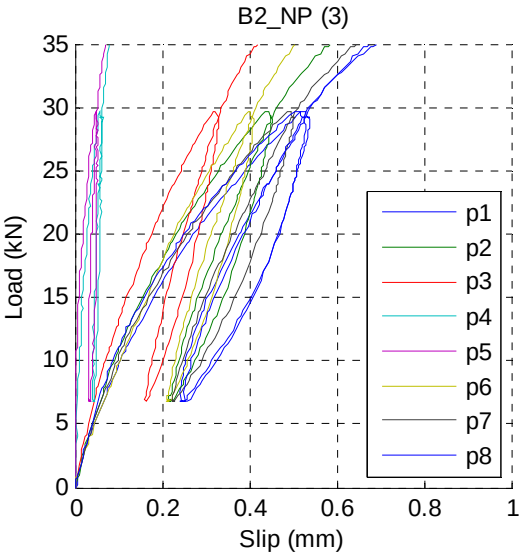
B2_NP (3)
Load (kN)
Slip (mm)
p1
p2
p3
p4
p5
p6
p7
p8

Series B3_NP+S (Double-sided nail plates and inclined screws combined)

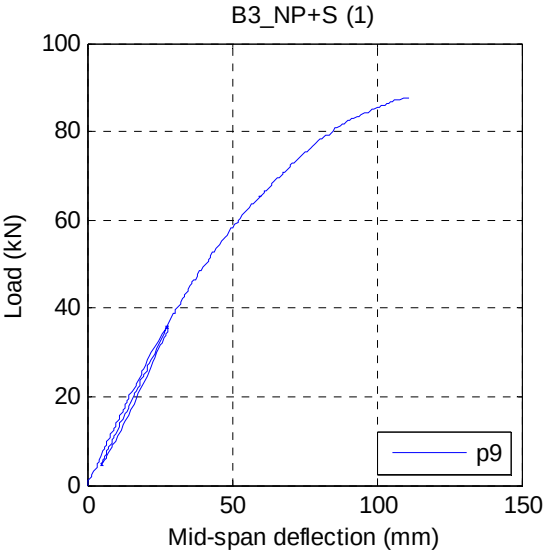

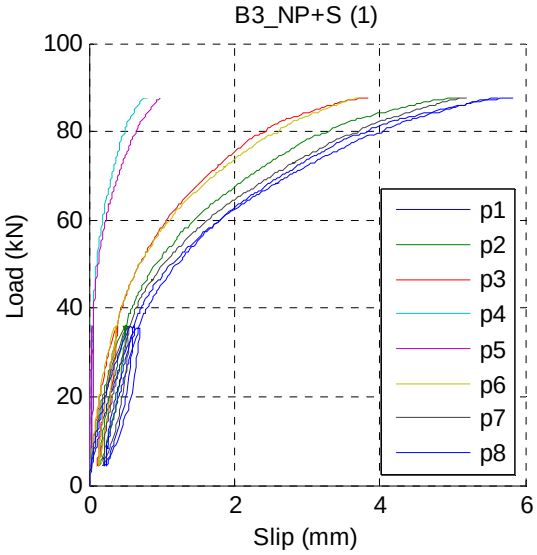

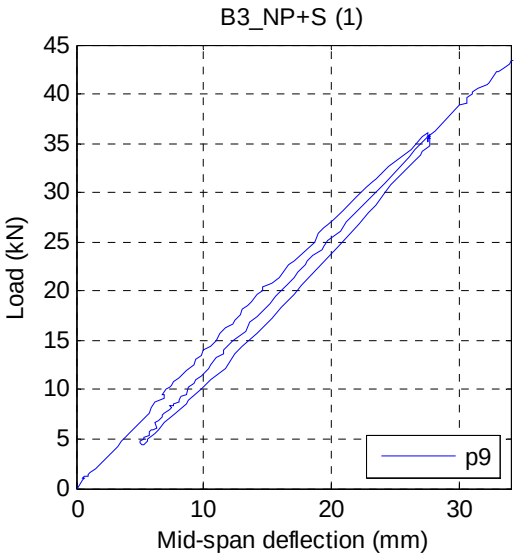

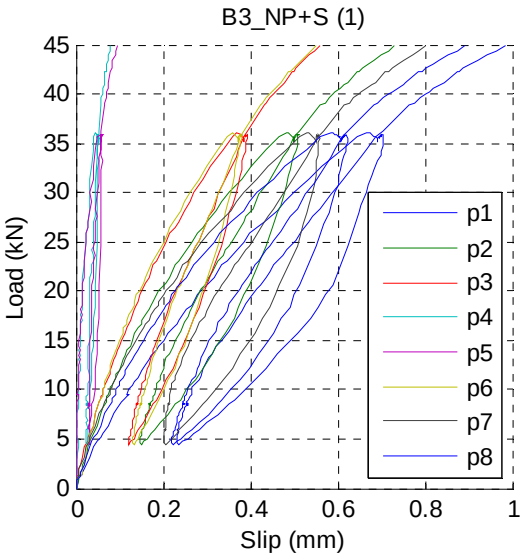

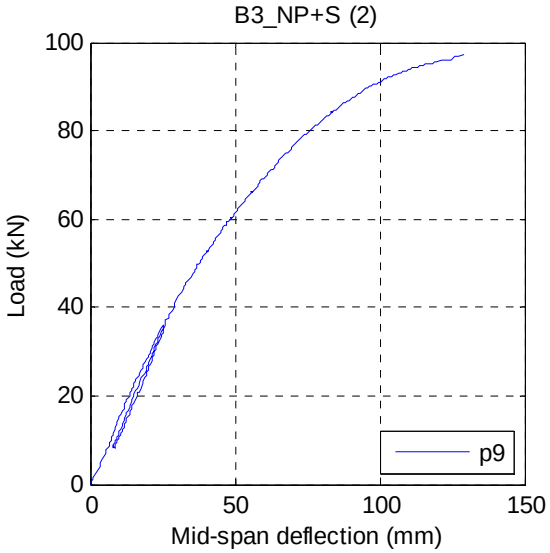
B3_NP+S (2)
Load (kN)
Mid-span deflection (mm)
p9

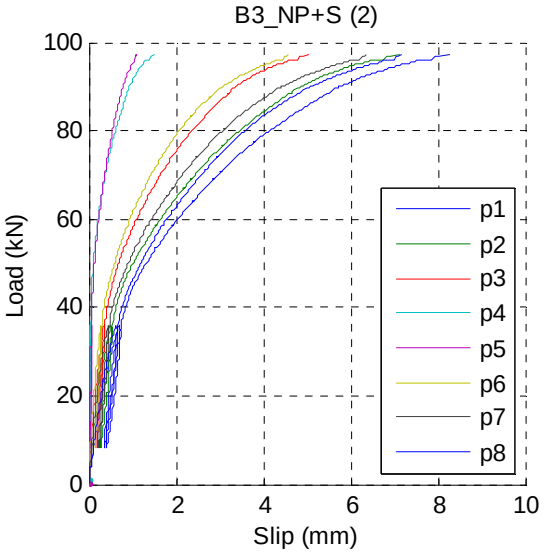
B3_NP+S (2)
Load (kN)
Slip (mm)
p1
p2
p3
p4
p5
p6
p7
p8

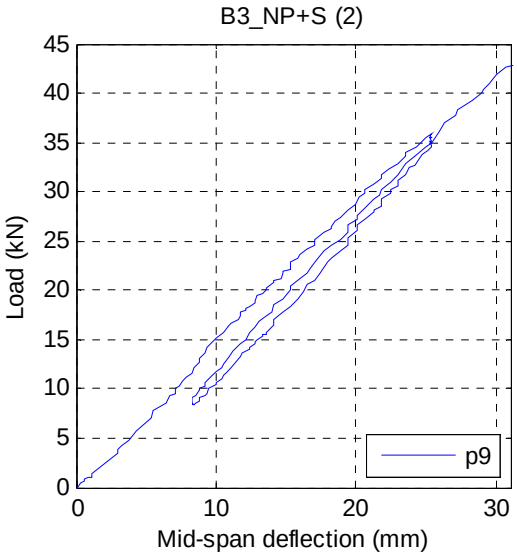
B3_NP+S (2)
Load (kN)
Mid-span deflection (mm)
p9

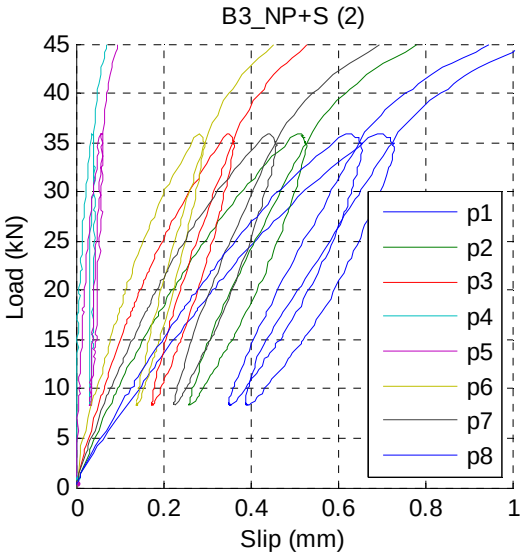
B3_NP+S (2)
Load (kN)
Slip (mm)
p1
p2
p3
p4
p5
p6
p7
p8

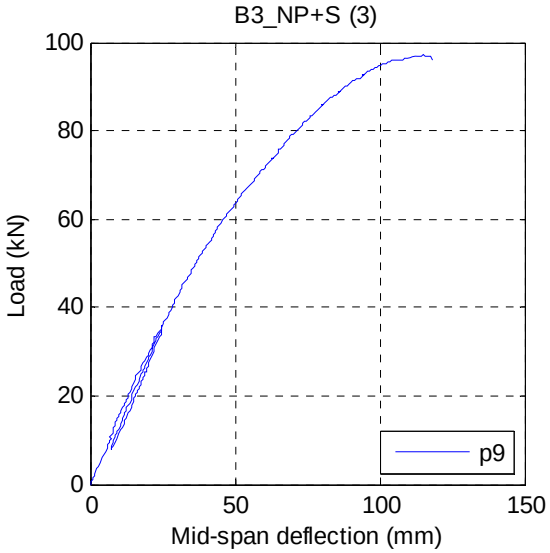
B3_NP+S (3)
Load (kN)
Mid-span deflection (mm)
p9

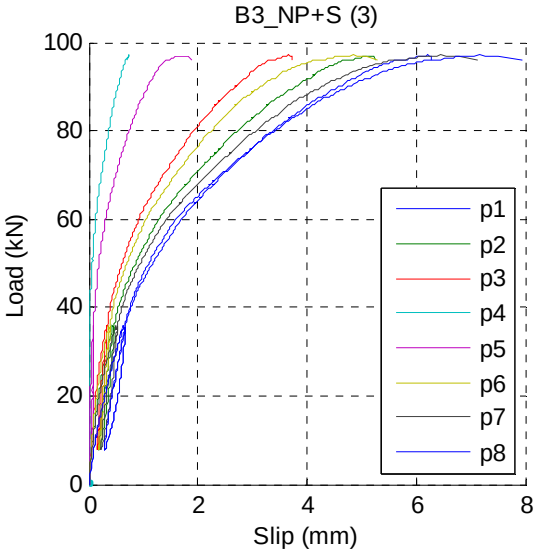
B3_NP+S (3)
Load (kN)
Slip (mm)
p1
p2
p3
p4
p5
p6
p7
p8

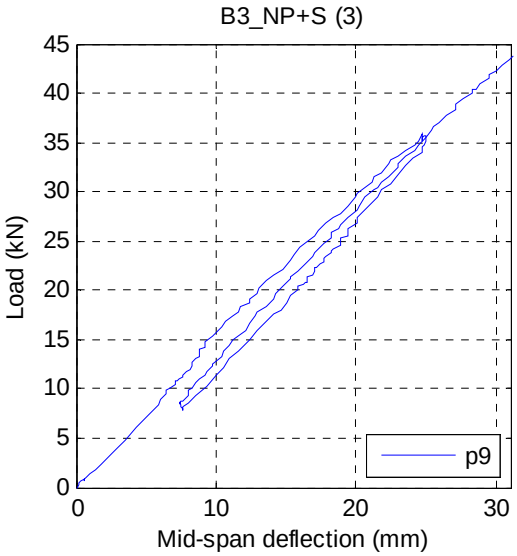
B3_NP+S (3)
Load (kN)
Mid-span deflection (mm)
p9

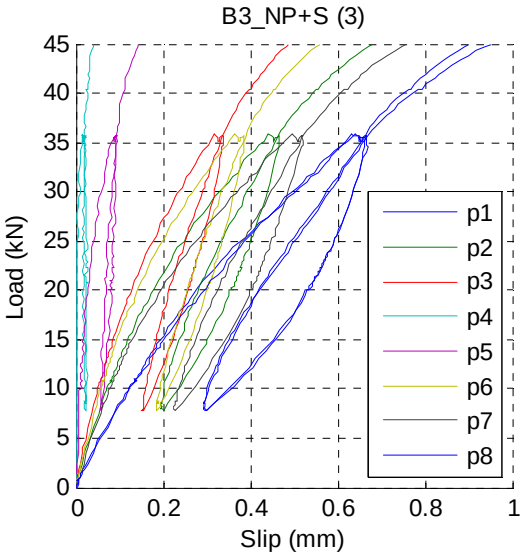
B3_NP+S (3)
Load (kN)
Slip (mm)
p1
p2
p3
p4
p5
p6
p7
p8

Series B4_SG (Screw-gluing)

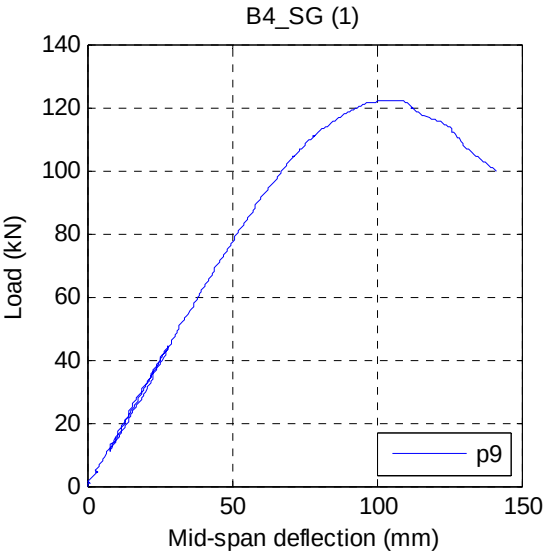

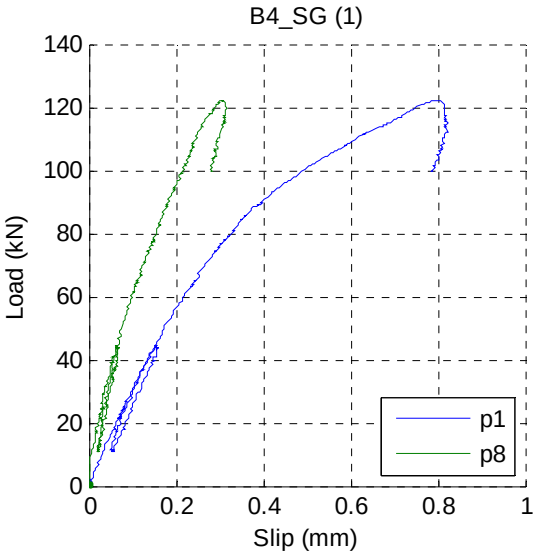

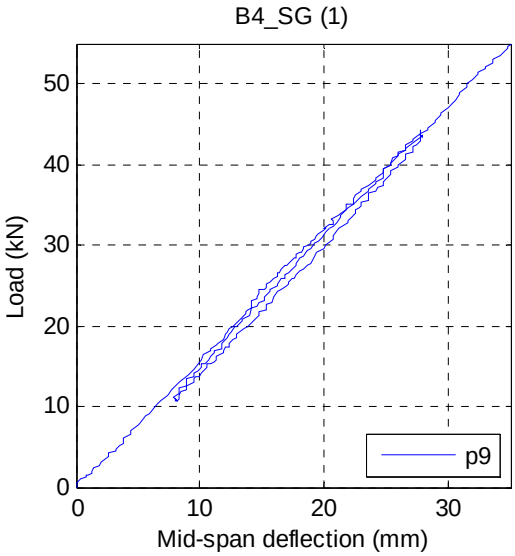

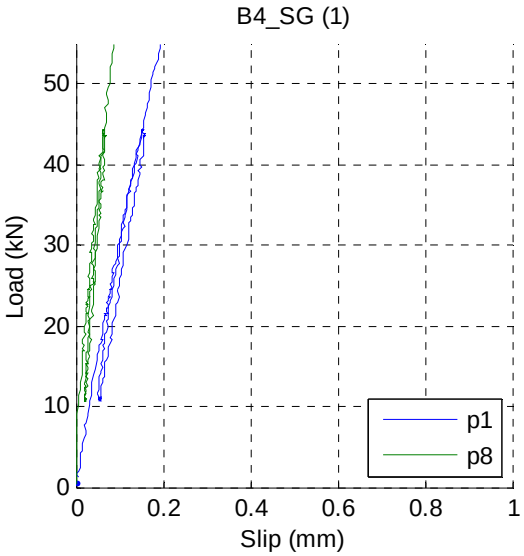

Appendix C: Tables of test results per test series

Notations

F_{est}	Estimated failure load (EN 26891)
F_{04}	= 0.4 × F_{est}
F_{01}	= 0.1 × F_{est}
$\delta_{01.Fest}$	Mid-span deflection at 0.1 × F_{est} (see loading procedure Fig. 15)
$\delta_{04.Fest}$	Mid-span deflection at 0.4 × F_{est} (see loading procedure Fig. 15)
$\delta_{14.Fest}$	Mid-span deflection at 0.4 × F_{est} (see loading procedure Fig. 15)
$\delta_{11.Fest}$	Mid-span deflection at 0.1 × F_{est} (see loading procedure Fig. 15)
$\delta_{21.Fest}$	Mid-span deflection at 0.1 × F_{est} (see loading procedure Fig. 15)
$\delta_{24.Fest}$	Mid-span deflection at 0.4 × F_{est} (see loading procedure Fig. 15)
$\delta_{06.Fmax}$	Mid-span deflection at 0.6 × F_{max} (see loading procedure Fig. 15)
$\delta_{08.Fmax}$	Mid-span deflection at 0.8 × F_{max} (see loading procedure Fig. 15)
δ_{Fmax}	Mid-span deflection at F_{max}
F_{max}	Maximum load
$EI_{04.Fest}$	Bending stiffness estimated between 0.1 × F_{est} and 0.4 × F_{est}
$\delta_{01.Fmax}$	Mid-span deflection at the load 0.1 × F_{max}
$\delta_{04.Fmax}$	Mid-span deflection at the load 0.4 × F_{max}
$EI_{04.Fmax}$	Bending stiffness estimated between 0.1 × F_{max} and 0.4 × F_{max}
$\delta_{sls/4}$	Mid-span deflection at the load (1/4) × F_{sls}
δ_{sls}	Mid-span deflection at the load F_{sls}
EI_{sls}	Bending stiffness estimated between (1/4) × F_{sls} and F_{sls}
$v_{sls.(1)}$	End slip at the load F_{sls} (measurement point 1)
$v_{sls.(8)}$	End slip at the load F_{sls} (measurement point 8)
δ_{uls}	Mid-span deflection at the load F_{uls}
EI_{uls}	Bending stiffness estimated between (1/4) × F_{uls} and F_{uls}
$v_{uls.(1)}$	End slip at the load F_{uls} (measurement point 1)
$v_{uls.(8)}$	End slip at the load F_{uls} (measurement point 8)
$\rho_{g,\omega}$	Density of the glulam at moisture content ω
$\rho_{g,0,\omega}$	Dry density of the glulam
ω_g	Moisture content of the glulam
$\rho_{c,\omega}$	Density of the CLT at moisture content ω
$\rho_{c,0,\omega}$	Dry density of the CLT
ω_c	Moisture content of the CLT

Series B1_S (Inclined screws only)

Test Series	**B1**						
Test specimen		**1**	**2**	**3**	**Mean**	**St.dev**	**cov(%)**
F_{est}	[kN]	75	75	75			
F_{04}	[kN]	30	30	30			
F_{01}	[kN]	7.5	7.5	7.5			
$\delta_{01.Fest}$	[mm]	6.840	8.220	7.655	7.572	0.694	9.163
$\delta_{04.Fest}$	[mm]	40.200	44.430	43.520	42.717	2.226	5.212
$\delta_{14.Fest}$	[mm]	40.790	45.890	44.700	43.793	2.668	6.093
$\delta_{11.Fest}$	[mm]	18.865	19.120	19.125	19.037	0.149	0.781
$\delta_{21.Fest}$	[mm]	17.950	18.580	18.450	18.327	0.333	1.815
$\delta_{24.Fest}$	[mm]	41.310	45.800	44.760	43.957	2.350	5.347
$\delta_{06.Fmax}$	[mm]	57.340	66.028	71.112	64.827	6.964	10.743
$\delta_{08.Fmax}$	[mm]	80.760	91.974	100.315	91.016	9.813	10.781
δ_{Fmax}	[mm]	104.740	146.540	148.830	133.370	24.821	18.610
F_{max}	[kN]	65.400	68.800	74.000	69.400	4.331	6.241
$EI_{04.Fest}$	[MN.m^2]	3.137	2.890	2.918	2.982	0.135	4.536
$\delta_{01.Fmax}$	[mm]	6.300	7.695	8.210	7.402	0.988	13.351
$\delta_{04.Fmax}$	[mm]	34.544	40.482	44.680	39.902	5.093	12.763
$EI_{04.Fmax}$	[MN.m^2]	3.231	2.928	2.832	2.997	0.209	6.959
$\delta_{sls/4}$	[mm]	2.316	3.020	2.993	2.776	0.399	14.358
δ_{sls}	[mm]	10.750	12.360	12.127	11.746	0.870	7.407
EI_{sls}	[MN.m^2]	4.385	3.959	4.049	4.131	0.224	5.431
$v_{sls.(1)}$	[mm]	0.614	0.967	0.619	0.733	0.202	27.597
$v_{sls.(8)}$	[mm]	0.608	0.614	0.668	0.630	0.033	5.245
δ_{uls}	[mm]	14.495	16.655	16.925	16.025	1.332	8.311
EI_{uls}	[MN.m^2]	4.337	3.869	3.838	4.015	0.279	6.951
$v_{uls.(1)}$	[mm]	0.956	1.451	1.049	1.152	0.263	22.837
$v_{uls.(8)}$	[mm]	1.012	0.942	1.034	0.996	0.048	4.823
$\rho_{g,\omega}$	[kg/m^3]	416	477	530	474	57.0	12.0
$\rho_{g,0,\omega}$	[kg/m^3]	367	420	464	417	48.4	11.6
ω_g	[%]	13.3	13.5	14.2	13.7	0.5	3.7
$\rho_{c,\omega}$	[kg/m^3]	425	472	469	455	26.3	5.8
$\rho_{c,0,\omega}$	[kg/m^3]	375	418	417	403	24.2	6.0
ω_c	[%]	13.2	13.0	12.5	12.9	0.3	2.6

Series B2_NP (Double-sided nail plates only)

Test Series	**B2**						
Test specimen		**1**	**2**	**3**	**Mean**	**St.dev**	**cov(%)**
F_{est}	[kN]	75	75	75			
F_{04}	[kN]	30	30	30			
F_{01}	[kN]	7.5	7.5	7.5			
$\delta_{01.Fest}$	[mm]	5.445	5.280	4.933	5.219	0.261	5.003
$\delta_{04.Fest}$	[mm]	22.470	22.310	20.850	21.877	0.893	4.081
$\delta_{14.Fest}$	[mm]	22.880	22.770	21.370	22.340	0.842	3.768
$\delta_{11.Fest}$	[mm]	8.005	7.675	7.300	7.660	0.353	4.605
$\delta_{21.Fest}$	[mm]	7.820	7.380	7.290	7.497	0.284	3.783
$\delta_{24.Fest}$	[mm]	22.897	22.600	21.305	22.267	0.846	3.801
$\delta_{06.Fmax}$	[mm]	45.159	45.088	44.360	44.869	0.442	0.986
$\delta_{08.Fmax}$	[mm]	67.740	68.418	66.216	67.458	1.128	1.672
δ_{Fmax}	[mm]	99.380	103.830	99.960	101.057	2.419	2.394
F_{max}	[kN]	85.600	85.800	90.800	87.400	2.946	3.371
$EI_{04.Fest}$	[MN.m^2]	6.148	6.146	6.576	6.290	0.248	3.938
$\delta_{01.Fmax}$	[mm]	6.477	6.344	6.392	6.404	0.068	1.054
$\delta_{04.Fmax}$	[mm]	26.970	26.676	26.652	26.766	0.177	0.662
$EI_{04.Fmax}$	[MN.m^2]	5.829	5.889	6.254	5.991	0.230	3.842
$\delta_{sls/4}$	[mm]	2.020	1.939	1.889	1.949	0.066	3.389
δ_{sls}	[mm]	7.820	7.622	7.300	7.581	0.262	3.462
EI_{sls}	[MN.m^2]	6.376	6.507	6.835	6.573	0.236	3.594
$v_{sls.(1)}$	[mm]	0.126	0.164	0.115	0.135	0.026	19.044
$v_{sls.(8)}$	[mm]	0.128	0.134	0.097	0.120	0.020	16.594
δ_{uls}	[mm]	10.313	10.408	9.635	10.118	0.421	4.163
EI_{uls}	[MN.m^2]	6.732	6.390	6.886	6.669	0.254	3.808
$v_{uls.(1)}$	[mm]	0.185	0.230	0.166	0.194	0.033	16.972
$v_{uls.(8)}$	[mm]	0.186	0.186	0.145	0.172	0.024	13.736
$\rho_{g,\omega}$	[kg/m^3]	418	428	468	438	26.3	6.0
$\rho_{g,0,\omega}$	[kg/m^3]	368	377	409	384	22.0	5.7
ω_g	[%]	13.7	13.8	14.3	13.9	0.3	2.4
$\rho_{c,\omega}$	[kg/m^3]	448	439	494	461	29.7	6.4
$\rho_{c,0,\omega}$	[kg/m^3]	396	389	438	408	26.3	6.5
ω_c	[%]	13.0	13.0	13.0	13.0	0.0	0.3

Series B3_NP+S (Double-sided nail plates and inclined screws combined)

Test Series	**B3**						
Test specimen		**1**	**2**	**3**	**Mean**	**St.dev**	**cov(%)**
F_{est}	[kN]	90	90	90			
F_{04}	[kN]	36	36	36			
F_{01}	[kN]	9	9	9			
$\delta_{01.Fest}$	[mm]	6.117	6.253	5.900	6.090	0.178	2.919
$\delta_{04.Fest}$	[mm]	27.060	24.940	24.497	25.499	1.370	5.373
$\delta_{14.Fest}$	[mm]	27.610	25.290	24.900	25.933	1.465	5.649
$\delta_{11.Fest}$	[mm]	8.620	8.370	7.825	8.272	0.407	4.915
$\delta_{21.Fest}$	[mm]	5.870	8.260	7.410	7.180	1.211	16.873
$\delta_{24.Fest}$	[mm]	27.550	25.556	24.930	26.012	1.368	5.260
$\delta_{06.Fmax}$	[mm]	43.449	46.259	44.312	44.674	1.439	3.222
$\delta_{08.Fmax}$	[mm]	67.107	72.006	68.362	69.158	2.545	3.680
δ_{Fmax}	[mm]	109.770	128.900	115.290	117.987	9.846	8.345
F_{max}	[kN]	87.600	97.200	97.200	94.000	5.543	5.896
$EI_{04.Fest}$	[MN.m^2]	5.997	6.721	6.754	6.491	0.428	6.590
$\delta_{01.Fmax}$	[mm]	6.215	7.070	6.466	6.584	0.439	6.673
$\delta_{04.Fmax}$	[mm]	26.682	27.884	27.175	27.247	0.604	2.218
$EI_{04.Fmax}$	[MN.m^2]	5.973	6.517	6.550	6.347	0.324	5.106
$\delta_{sls/4}$	[mm]	1.934	2.283	1.973	2.063	0.191	9.255
δ_{sls}	[mm]	7.580	7.530	7.050	7.387	0.293	3.962
EI_{sls}	[MN.m^2]	6.550	7.047	7.283	6.960	0.374	5.375
$v_{sls.(1)}$	[mm]	0.135	0.156	0.132	0.141	0.013	9.274
$v_{sls.(8)}$	[mm]	0.101	0.134	0.136	0.124	0.020	15.894
δ_{uls}	[mm]	10.160	9.363	9.015	9.513	0.587	6.170
EI_{uls}	[MN.m^2]	6.544	7.670	7.711	7.308	0.663	9.066
$v_{uls.(1)}$	[mm]	0.191	0.212	0.183	0.195	0.015	7.668
$v_{uls.(8)}$	[mm]	0.147	0.185	0.193	0.175	0.025	14.044
$\rho_{g,\omega}$	[kg/m^3]	423	486	452	454	31.5	6.9
$\rho_{g,0,\omega}$	[kg/m^3]	371	426	397	398	27.7	7.0
ω_g	[%]	14.2	14.1	13.8	14.0	0.2	1.2
$\rho_{c,\omega}$	[kg/m^3]	456	481	453	463	15.3	3.3
$\rho_{c,0,\omega}$	[kg/m^3]	402	427	402	410	14.6	3.6
ω_c	[%]	13.3	12.5	12.8	12.9	0.4	2.9

Series B4_SG (Screw-gluing)

Test Series	**B4**	
Test specimen		**1**
F_{est}	[kN]	110
F_{04}	[kN]	44
F_{01}	[kN]	11
$\delta_{01.Fest}$	[mm]	6.903
$\delta_{04.Fest}$	[mm]	27.690
$\delta_{14.Fest}$	[mm]	27.760
$\delta_{11.Fest}$	[mm]	8.140
$\delta_{21.Fest}$	[mm]	9.480
$\delta_{24.Fest}$	[mm]	27.740
$\delta_{06.Fmax}$	[mm]	47.160
$\delta_{08.Fmax}$	[mm]	65.536
δ_{Fmax}	[mm]	102.220
F_{max}	[kN]	122.200
$EI_{04.Fest}$	[MN.m^2]	7.385
$\delta_{01.Fmax}$	[mm]	7.836
$\delta_{04.Fmax}$	[mm]	30.891
$EI_{04.Fmax}$	[MN.m^2]	7.397
$\delta_{sls/4}$	[mm]	1.904
δ_{sls}	[mm]	6.750
EI_{sls}	[MN.m^2]	7.632
$v_{sls.(1)}$	[mm]	0.031
$v_{sls.(8)}$	[mm]	0.006
δ_{uls}	[mm]	9.093
EI_{uls}	[MN.m^2]	7.315
$v_{uls.(1)}$	[mm]	0.045
$v_{uls.(8)}$	[mm]	0.016
$\rho_{g,\omega}$	[kg/m^3]	489
$\rho_{g,0,\omega}$	[kg/m^3]	428
ω_g	[%]	14.2
$\rho_{c,\omega}$	[kg/m^3]	467
$\rho_{c,0,\omega}$	[kg/m^3]	414
ω_c	[%]	12.7

Acknowledgements

The centre for Lean Wood Engineering, the Swedish governmental agency for innovation systems (VINNOVA), Stora Enso Timber, the County Administrative Board in Norrbotten under Grant number 303-2602-13 (174311); the Regional Council of Västerbotten under Grant number REGAC-2013-000133 (00179026); and the European Union's Structural Funds - The Regional Fund under Grant number 2013-000828 (174106) are acknowledged for their financial support to this research.
Ari Kevarinmäki is acknowledged for his comments and assistance when carrying out the tests at VTT Expert Services laboratories in Finland. Sepa Oy and SFS Intec are acknowledged for providing the mechanical fasteners used in this test program.

References

[1] Jacquier N. Shear tests on glulam-CLT joints with double-sided punched metal plate fasteners and inclined screws. Luleå Univeristy of Technology2014.
[2] Jacquier N, Girhammar UA. Tests on glulam-CLT shear connections with double-sided punched metal plate fasteners and inclined screws. Construction and Building Materials. 2014;72:444-57.
[3] Österreichisches Institut für Bautechnik (OIB) MoE. European technical approval ETA-12/0063 - SFS self-tapping screws WT. 2012.
[4] SFS intec. WFD-traebyggnadsskruv med kombinationsdrivning för sammanfogning av trä.
[5] European Committe for Standardization (CEN). SS-EN 1194:1999 - Glued laminated timber - Strength classes and determination of characteristic values. Swedish Institute for Standards (SIS); 1999.
[6] DIBT. European Technical Approval ETA-08/0271. Deutsches Institut für Bautechnik; 2009.
[7] European Committe for Standardization (CEN). SS-EN 408:2010+A1:2012 Timber structures - Structural timber and glued laminated timber - Determination of some physical and mechanical properties. Swedish Institute for Standards (SIS); 2012.
[8] Deutsches Institut für Bautechnik (DIBt). European Technical Approval ETA-08/0271 - CLT - Cross Laminated Timber. In: European Organisation for Technical Approvals (EOTA), editor. ETA-08/02712011. p. 17.
[9] European Committe for Standardization (CEN). EN 1995-1-1:2004 (E). Eurocode 5 Design of timber structures: CEN; 2004.
[10] SFS-EN 1995-1-1 EUROCODE 5: Design of timber structures. 2004.
[11] Gagnon S, Pirvu C. CLT Handbook Cross-Laminated Timber - Canadian Edition. Québec: FP Innovations; 2011.
[12] Yeoh D, Fragiacomo M. The design of a semi-prefabricated LVL-concrete composite floor. Advances in Civil Engineering. 2012;2012.
[13] Finnish Ministry of the Environment. National Annex To Standard SFS-EN 1995-1-1 EUROCODE 5: Design of Timber Structures Part 1-1: Common rules and rules for buildings (Unofficial translation). 2007.
[14] RIL 205-1-2009 korjaukset 30.1.2012. 2012.
[15] European Committe for Standardization (CEN). EN 26891:1991 - Timber structures - Joints made with mechanical fasteners - General principles for the determination of strength and deformation characteristics. 1991.
[16] European Committe for Standardization (CEN). EN 338: Structural Timber - Strenght classes. Brussels2009.
[17] Dimensionering genom provning. Karlskrona: Boverket; 1994.